

Building and evaluation of a PBPK model for clarithromycin in healthy adults

Version	2.0-OSP12.1
based on <i>Model Snapshot</i> and <i>Evaluation Plan</i>	https://github.com/Open-Systems-Pharmacology/Clarithromycin-Model/releases/tag/v2.0
OSP Version	12.1
Qualification Framework Version	3.3

This evaluation report and the corresponding PK-Sim project file are filed at:

<https://github.com/Open-Systems-Pharmacology/OSP-PBPK-Model-Library/>

Table of Contents

- [1 Introduction](#)
- [2 Methods](#)
 - [2.1 Modeling Strategy](#)
 - [2.2 Data](#)
 - [2.3 Model Parameters and Assumptions](#)
- [3 Results and Discussion](#)
 - [3.1 Final input parameters](#)
 - [3.2 Diagnostics Plots](#)
 - [3.3 Concentration-Time Profiles](#)
 - [3.3.1 Model Building](#)
 - [3.3.2 Model Verification](#)
- [4 Conclusion](#)
- [5 References](#)

1 Introduction

Clarithromycin is a widely prescribed macrolide antibiotic and a substrate and mechanism-based inactivator of CYP3A4. Furthermore, clarithromycin is a substrate and inhibitor of P-gp and an inhibitor of OATP1B1 and OATP1B3 ([Eberl 2007](#), [Seithel 2007](#)). Clarithromycin has been proposed as one of the best alternative CYP3A4 inhibitors for clinical DDI studies to avoid further use of ketoconazole.

Objectives were to develop a fully mechanistic PBPK model for clarithromycin, describing its metabolism by CYP3A4 and its mechanism-based inactivation of the respective enzyme as well as its inhibition of P-gp.

The presented clarithromycin model was developed by Moj et al. ([Moj 2017](#)) and revised by Hanke et al. ([Hanke 2018](#)).

2 Methods

2.1 Modeling Strategy

The general workflow for building an adult PBPK model has been described by Kuepfer et al. ([Kuepfer 2016](#)). Relevant information on the anthropometry (height, weight) was gathered from the respective clinical study, if reported. Information on physiological parameters (e.g. blood flows, organ volumes, hematocrit) in adults was gathered from the literature and has been incorporated in PK-Sim® as described previously ([Willmann 2007](#)). The applied activity and variability of plasma proteins and active processes that are integrated into PK-Sim® are described in the publicly available 'PK-Sim® Ontogeny Database Version 7.3' ([PK-Sim Ontogeny Database Version 7.3](#)).

A typical European individual was used for the development of the clarithromycin model. The relative tissue-specific expression of CYP3A4 was implemented in accordance with literature information using the PK-Sim expression database RT-PCR profile. Enterohepatic recirculation was enabled as it is active under physiological conditions.

Unknown parameters (see [Section 2.3.4](#)) were identified using the Parameter Identification module provided in PK-Sim®.

The model was then verified by simulating the PK of additional clinical studies including a dose range of 100 to 1200 mg administered as single dose or as multiple doses.

Details about input data (physicochemical, *in vitro* and clinical) can be found in [Section 2.2](#).

Details about the structural model and its parameters can be found in [Section 2.3](#).

2.2 Data

2.2.1 In vitro / physicochemical Data

A literature search was performed to collect available information on physiochemical properties of clarithromycin. The obtained information from literature is summarized in the table below.

Parameter	Unit	Value	Source	Description
MW	g/mol	747.95	drugbank.ca	Molecular weight
pK _a (base)		8.99	McFarland 1997	Acid dissociation constant
Solubility (pH)	mg/L	12170 (2.4)	Salem 2003	Solubility
logP		2.3	Lappin 2011	Partition coefficient between octanol and water
fu	%	28.0	Davey 1991	Fraction unbound in plasma
	%	30.0	Chu 1993b	Fraction unbound in plasma
	%	40.0	Noreddin 2002	Fraction unbound in plasma
CYP3A4 K _m	μmol/L	48.7	Rodrigues 1997	Michaelis-Menten constant for CYP3A4 metabolism
CL _{ren}	L/h	6.66 - 12.8 ^a	Rodvold 1999	Renal clearance
CYP3A4 K _i	μmol/L	2.25	Polasek 2006	Conc. for half-maximal inactivation measured in recombinant CYP3A4
	μmol/L	29.5	Polasek 2006	Conc. for half-maximal inactivation measured in human liver microsomes
	μmol/L	41.4	Ito 2003	Conc. for half-maximal inactivation measured in human liver microsomes for α-hydroxylation of midazolam
	μmol/L	37.0	Ito 2003	Conc. for half-maximal inactivation measured in human liver microsomes for 4-hydroxylation of midazolam
	μmol/L	5.49	Mayhew 2000	Conc. for half-maximal inactivation measured in human liver microsomes
CYP3A4 k _{inact}	1/min	0.04	Polasek 2006	Maximum inactivation rate measured in recombinant CYP3A4
	1/min	0.05	Polasek 2006	Maximum inactivation rate measured in human liver microsomes
	1/min	0.0423	Ito 2003	Maximum inactivation rate measured in human liver microsomes for α-hydroxylation of midazolam
	1/min	0.0459	Ito 2003	Maximum inactivation rate measured in human liver microsomes for 4-hydroxylation of midazolam
	1/min	0.072	Mayhew 2000	Maximum inactivation rate measured in human liver microsomes
P-gp K _i	μmol/L	4.1	Eberl 2007	Conc. for half-maximal inhibition

Parameter	Unit	Value	Source	Description
OATP1B1 IC ₅₀	μmol/L	5.3 ± 1.3 ^b	Vermeer 2016	Half-maximal inhibitory concentration
OATP1B3 IC ₅₀	μmol/L	14 ± 2 ^b	Vermeer 2016	Half-maximal inhibitory concentration

^a denotes range of reported values

^b denotes mean ± standard error of the mean of the measurements (two assays, each performed in triplicate)

2.2.2 Clinical Data

A literature search was performed to collect available clinical data on clarithromycin in healthy adults. The clarithromycin model was developed using 17 clinical studies covering a dosing range from 100 to 1200 mg.

2.2.2.1 Model Building

The following studies were used for model building (training data):

Publication	Arm / Treatment / Information used for model building
Chu 1992b	Healthy subjects with intravenous infusion of 250 mg over 45 min
Chu 1993a	Healthy subjects with oral administration of 250 or 500 mg as single dose or twice daily for 5 days

2.2.2.2 Model Verification

The following studies were used for model verification (test data):

Publication	Arm / Treatment / Information used for model building
Chu 1992a	Healthy Subjects with oral administration of single doses ranging from 100 to 1200 mg
Kees 1995	Healthy subjects with oral administration of 250 or 500 mg as single or multiple dose
Rengelshausen 2003	Oral administration of 250 mg twice a day for 1.5 days
Abduljalil 2009	Oral administration of 500 mg twice a day for 3.5 days

2.3 Model Parameters and Assumptions

2.3.1 Absorption

The specific intestinal permeability was optimized during parameter identification to accurately describe the absorption of clarithromycin after oral administration.

2.3.2 Distribution

Values for lipophilicity and fraction unbound in plasma were fixed to literature values (namely to 2.3 ([Lappin 2011](#)) and 0.30 ([Chu 1993b](#)) for lipophilicity and fraction unbound, respectively).

It was not possible to adequately describe the observed plasma concentration-time profile after intravenous administration using standard input parameters (e.g. lipophilicity) and calculation methods. Simulated concentration-time profiles overestimated C_{\max} and underestimated the observed data for time to C_{\max} (T_{\max}). According to literature data, clarithromycin accumulates in mononuclear and polymorphonuclear leukocytes, probably via active transport ([Ishiguro 1989](#)). Implementing this process in the model improved the model fit significantly. Due to limited knowledge on this active transport, this process was technically implemented in the model by adjusting the permeability of clarithromycin across the membrane of the red blood cells (`P (blood cells->plasma)` and `P (plasma->blood cells)`).

After testing the available organ-plasma partition coefficient and cell permeability calculation methods built in PK-Sim, observed clinical data was best described by choosing the partition coefficient calculation by `Rodgers and Rowland` and cellular permeability calculation by `PK-Sim Standard`.

2.3.3 Metabolism and Elimination

Metabolism was described using Michaelis-Menten kinetics, while the Michaelis-Menten constant K_m was taken from in-vitro experiments from literature and the turnover rate k_{cat} was optimized during parameter identification.

K_i and k_{inact} to describe the mechanism-based inhibition of CYP3A4 were optimized during parameter identification.

A kidney plasma clearance was implemented to describe the renal elimination of clarithromycin. The specific renal clearance was optimized during parameter identification.

2.3.4 Automated Parameter Identification

This is the result of the final parameter identification.

Model Parameter	Optimized Value	Unit
<code>kcat</code> (CYP3A4)	76.5	1/min
<code>Specific clearance</code> in process renal clearance	0.87	1/min
<code>Specific intestinal permeability</code>	1.23 E-6	dm/min
<code>P (plasma->blood cells)</code>	3.62 E-5	dm/min
<code>P (blood cells->plasma)</code>	1.04 E-6	dm/min
<code>K_kinact_half</code> (K_i)	6.04	$\mu\text{mol/L}$
<code>kinact</code> (k_{inact})	0.04	1/min

3 Results and Discussion

The PBPK model for clarithromycin was developed and verified with clinical pharmacokinetic data.

The model was evaluated covering data from studies including in particular

- intravenous and oral administrations
- a dose range of 100 mg to 1200 mg
- single and multiple doses

The model quantifies metabolism via CYP3A4, including also the mechanism-based inhibition of the respective enzyme, as well as elimination via kidney. The model also includes inhibition of P-gp.

The next sections show:

1. the final model parameters for the building blocks: [Section 3.1](#).
2. the overall goodness of fit: [Section 3.2](#).
3. simulated vs. observed concentration-time profiles for the clinical studies used for model building and for model verification: [Section 3.3](#).

3.1 Final input parameters

The compound parameter values of the final PBPK model are illustrated below.

Compound: Clarithromycin

Parameters

Name	Value	Value Origin	Alternative	Default
Solubility at reference pH	12.17 mg/ml	Publication-Salem 2003	Measurement	True
Reference pH	2.4	Publication-Salem 2003	Measurement	True
Lipophilicity	2.3 Log Units	Publication-Lappin 2011	Measurement	True
Fraction unbound (plasma, reference value)	0.3	Publication-Chu 1993	Measurement	True
Specific intestinal permeability (transcellular)	1.23E-06 dm/min	Parameter Identification-optimized	fit	True
Is small molecule	Yes			
Molecular weight	747.9534 g/mol			
Plasma protein binding partner	Albumin			

Calculation methods

Name	Value
Partition coefficients	Rodgers and Rowland
Cellular permeabilities	PK-Sim Standard

Processes

Metabolizing Enzyme: CYP3A4-fit

Molecule: CYP3A4

Parameters

Name	Value	Value Origin
In vitro Vmax for liver microsomes	0 pmol/min/mg mic. protein	
Km	48.7 µmol/l	Publication-Rodrigues 1997
kcat	76.5 1/min	Parameter Identification

Systemic Process: Renal Clearances-fitted

Species: Human

Parameters

Name	Value	Value Origin
Body weight	71.5 kg	Unknown
Blood flow rate (kidney)	1.31 l/min	Unknown
Fraction unbound (experiment)	0.4	
Plasma clearance	1.75 ml/min/kg	

Inhibition: P-gp-Eberl (2007)

Molecule: P-gp

Parameters

Name	Value	Value Origin
Ki	4.1 µmol/l	Publication-Eberl 2007

Inhibition: CYP3A4-fitted

Molecule: CYP3A4

Parameters

Name	Value	Value Origin
kinact	0.04 1/min	
K_kinact_half	6.04 µmol/l	

Inhibition: OATP1B1-Vermeer 2016

Molecule: OATP1B1

Parameters

Name	Value	Value Origin
Ki	5.3 µmol/l	Publication-Vermeer 2016

Inhibition: OATP1B3-Vermeer 2016

Molecule: OATP1B3

Parameters

Name	Value	Value Origin
Ki	14 µmol/l	Publication-Vermeer 2016

Formulation: Tablet Clarithromycin

Type: Weibull

Parameters

Name	Value	Value Origin
Dissolution time (50% dissolved)	5 min	
Lag time	0 min	
Dissolution shape	2.9	
Use as suspension	No	

3.2 Diagnostics Plots

Below you find the goodness-of-fit visual diagnostic plots for the PBPK model performance of all data used presented in [Section 2.2.2](#).

The first plot shows simulated versus observed plasma concentrations, the second weighted residuals versus time.

Table 3-1: GMFE for Goodness of fit plot for concentration in plasma

Group	GMFE
model building	1.21
model evaluation	1.62
All	1.58

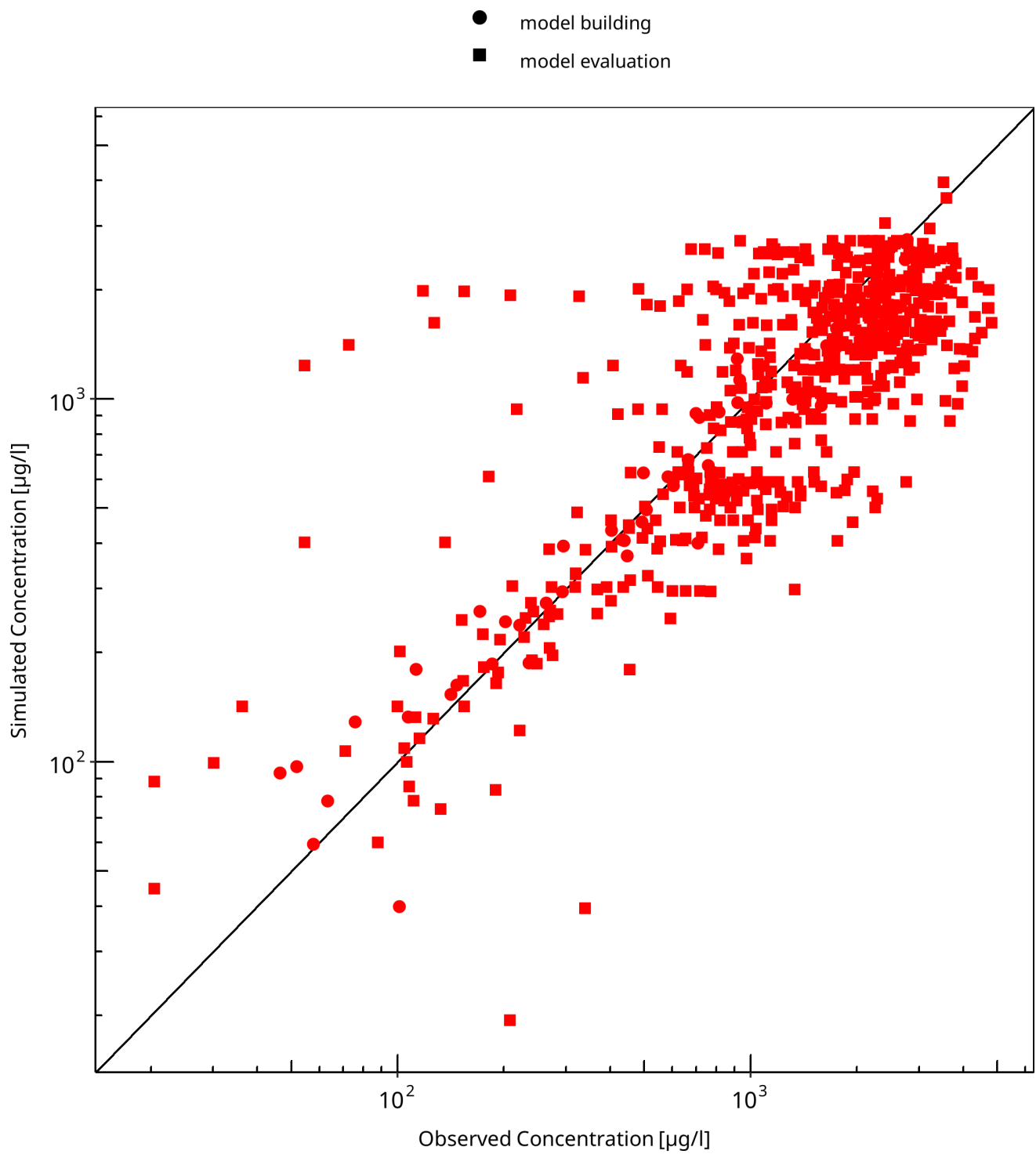


Figure 3-1: Goodness of fit plot for concentration in plasma

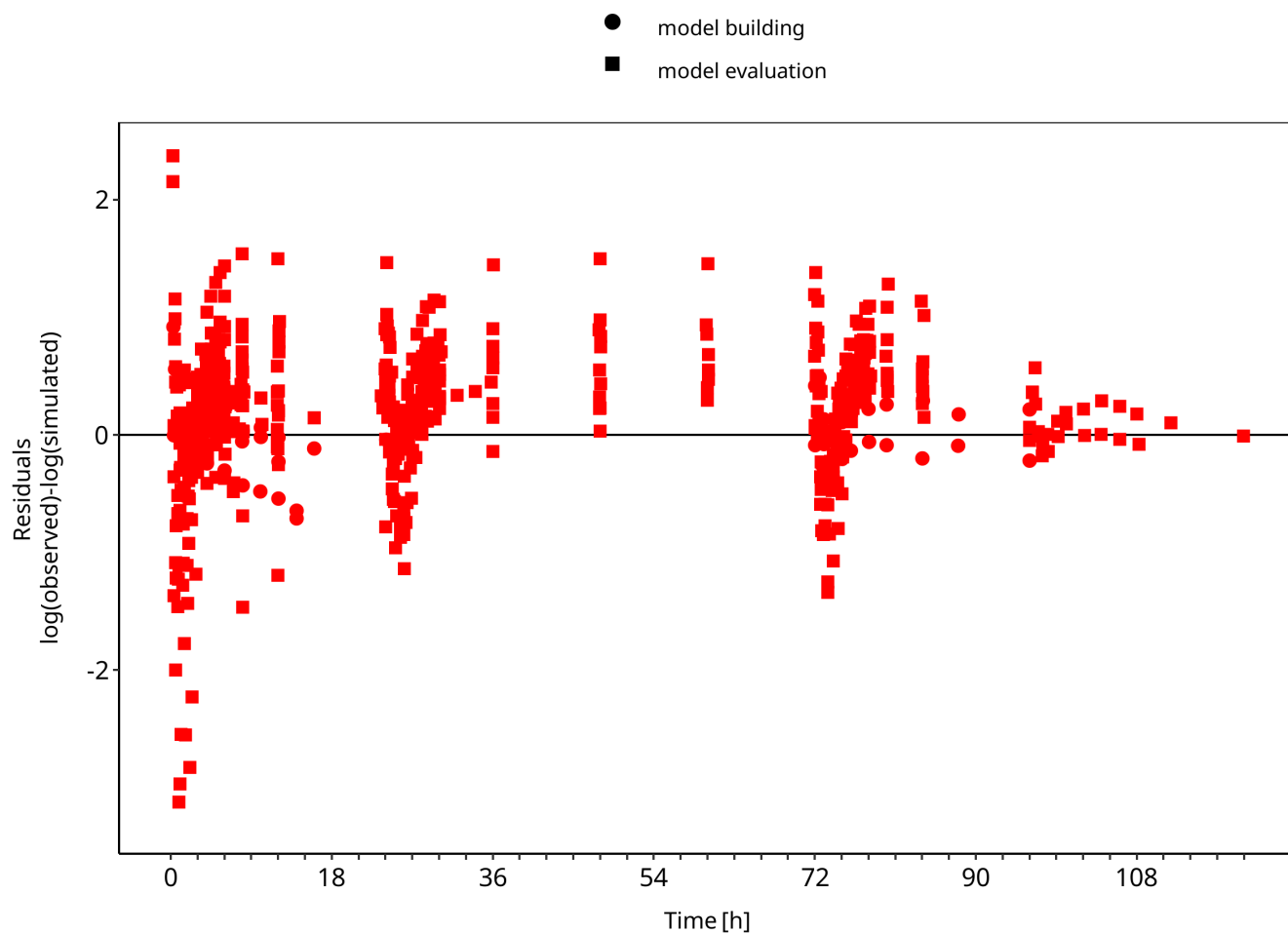


Figure 3-2: Goodness of fit plot for concentration in plasma

3.3 Concentration-Time Profiles

Simulated versus observed concentration-time profiles of all data listed in [Section 2.2.2](#) are presented below.

3.3.1 Model Building

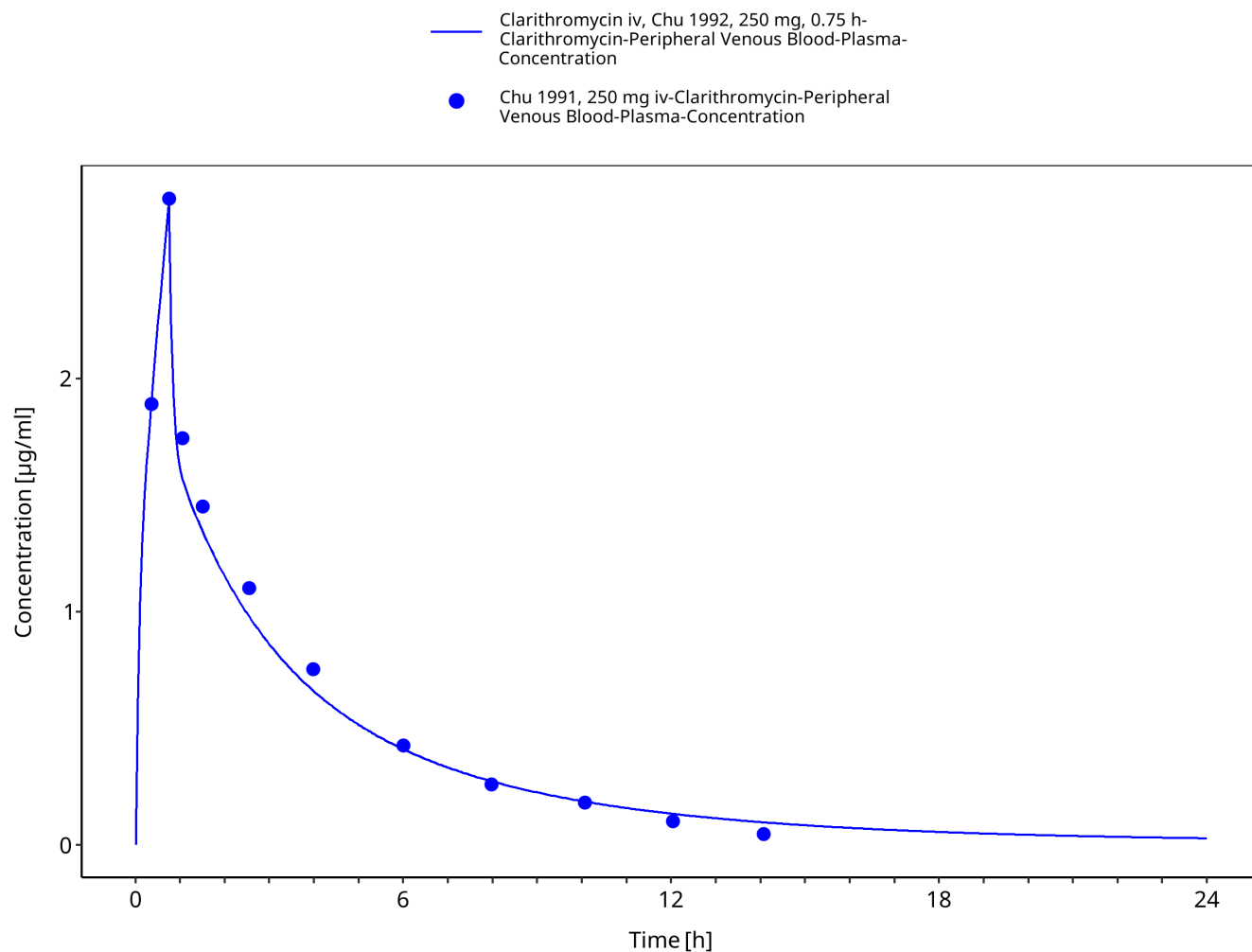


Figure 3-3: Time Profile Analysis

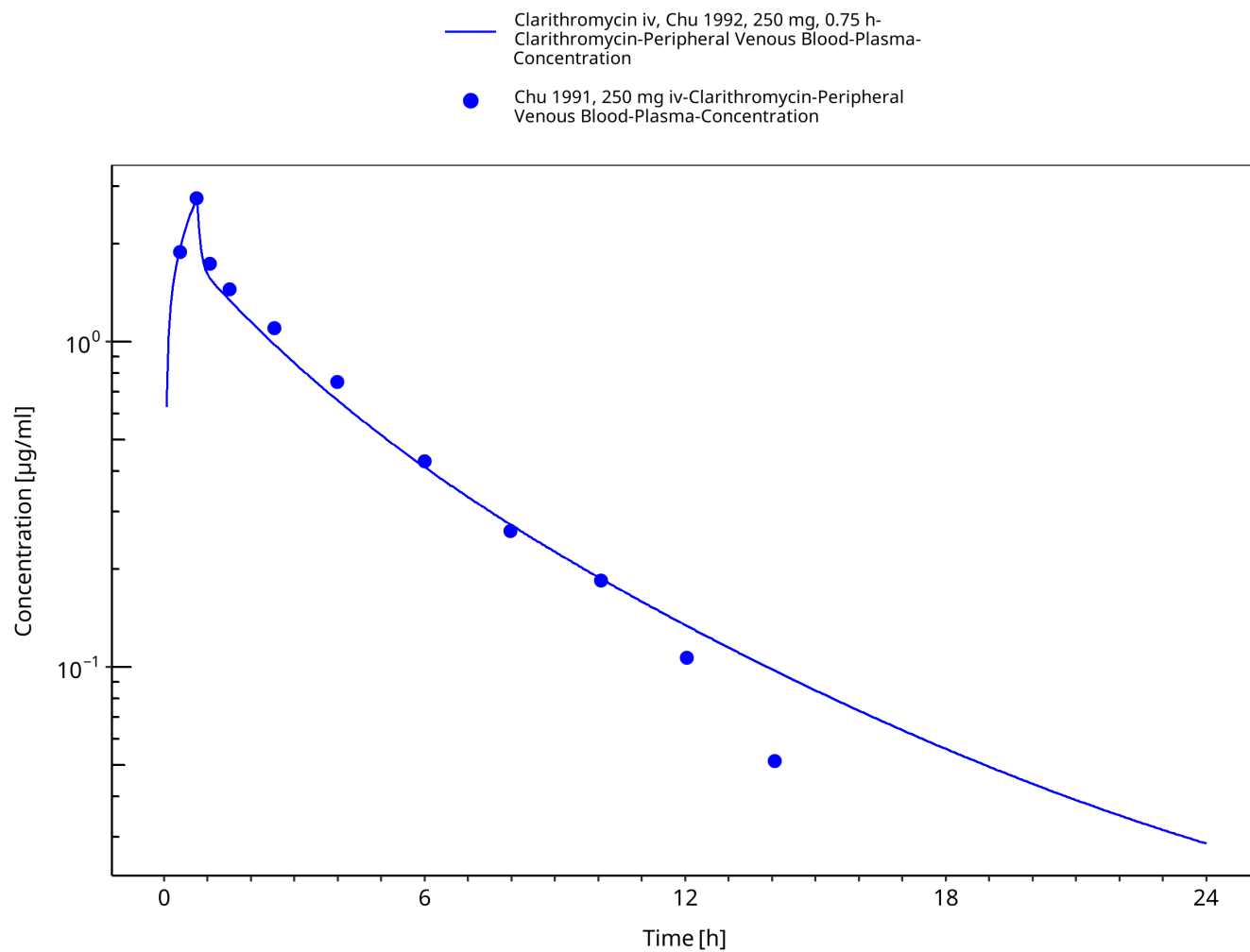


Figure 3-4: Time Profile Analysis 1

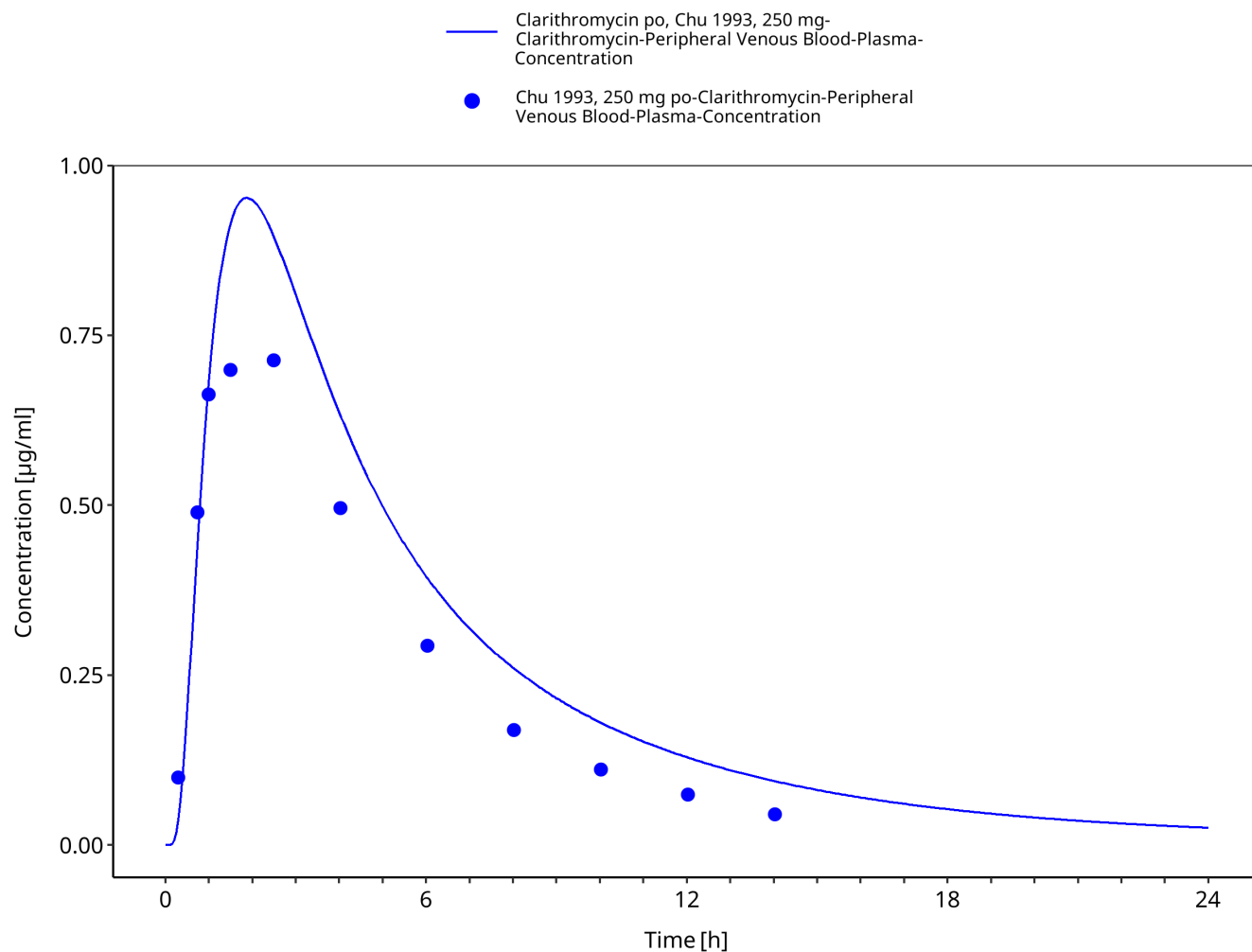


Figure 3-5: Time Profile Analysis

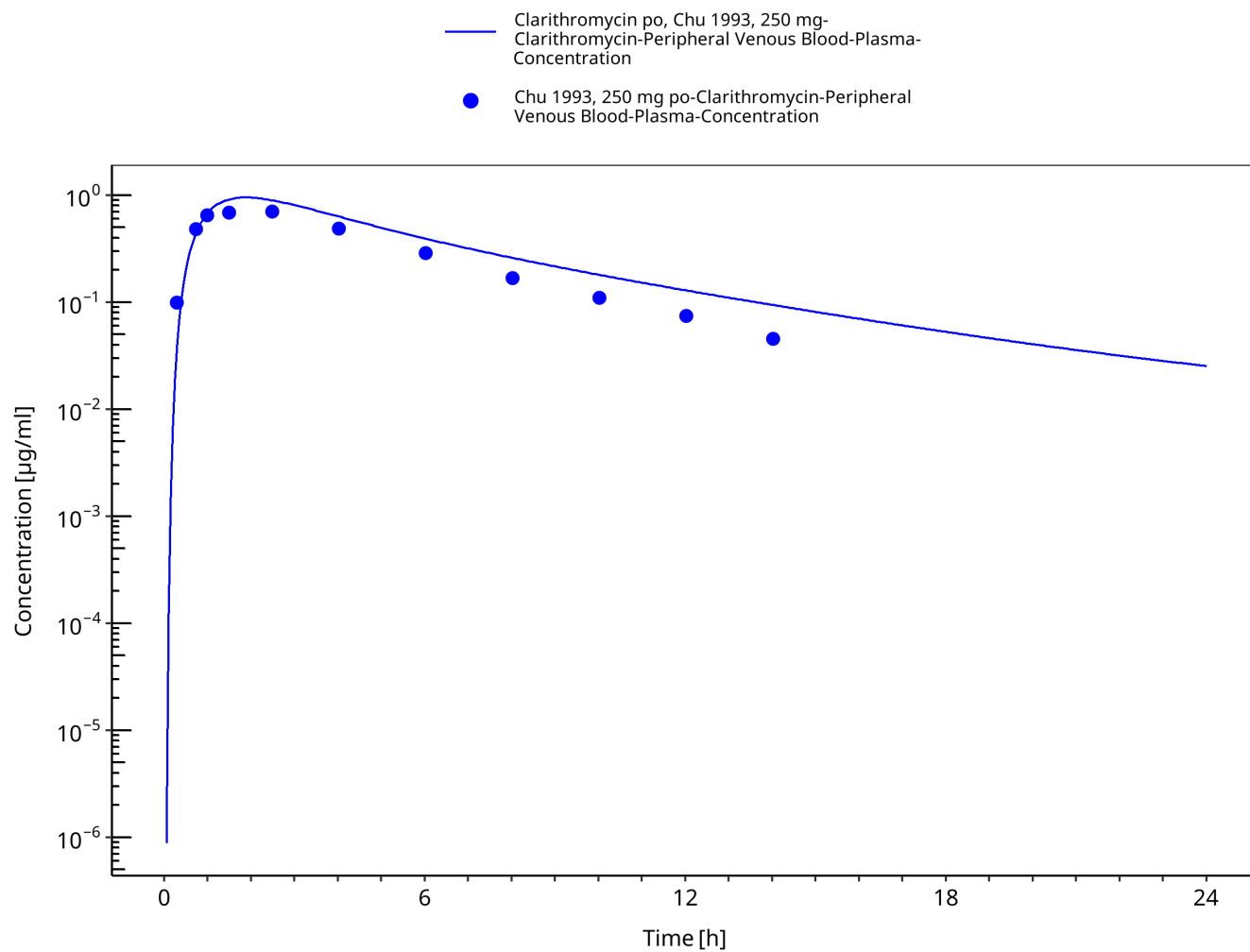


Figure 3-6: Time Profile Analysis 1

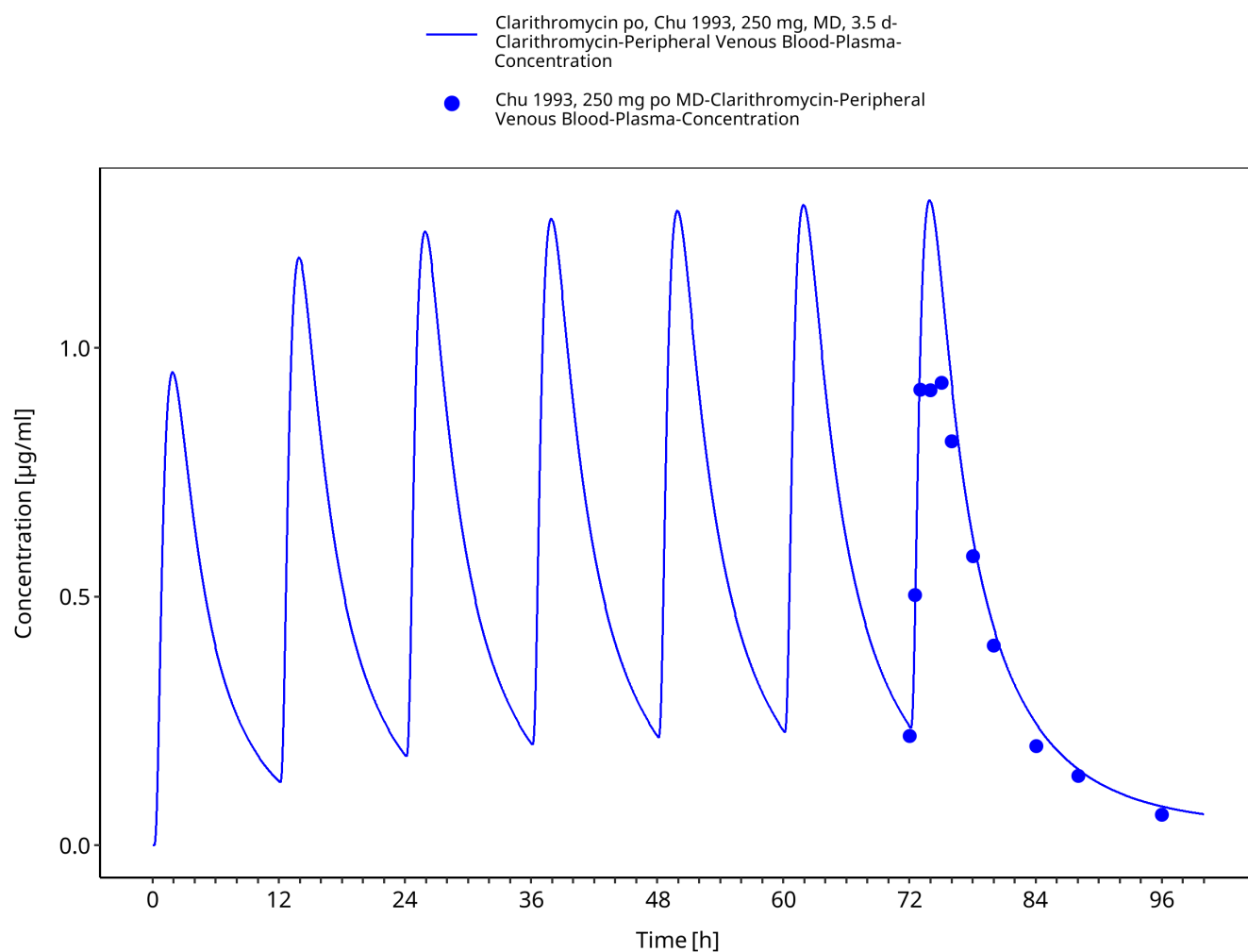


Figure 3-7: Time Profile Analysis

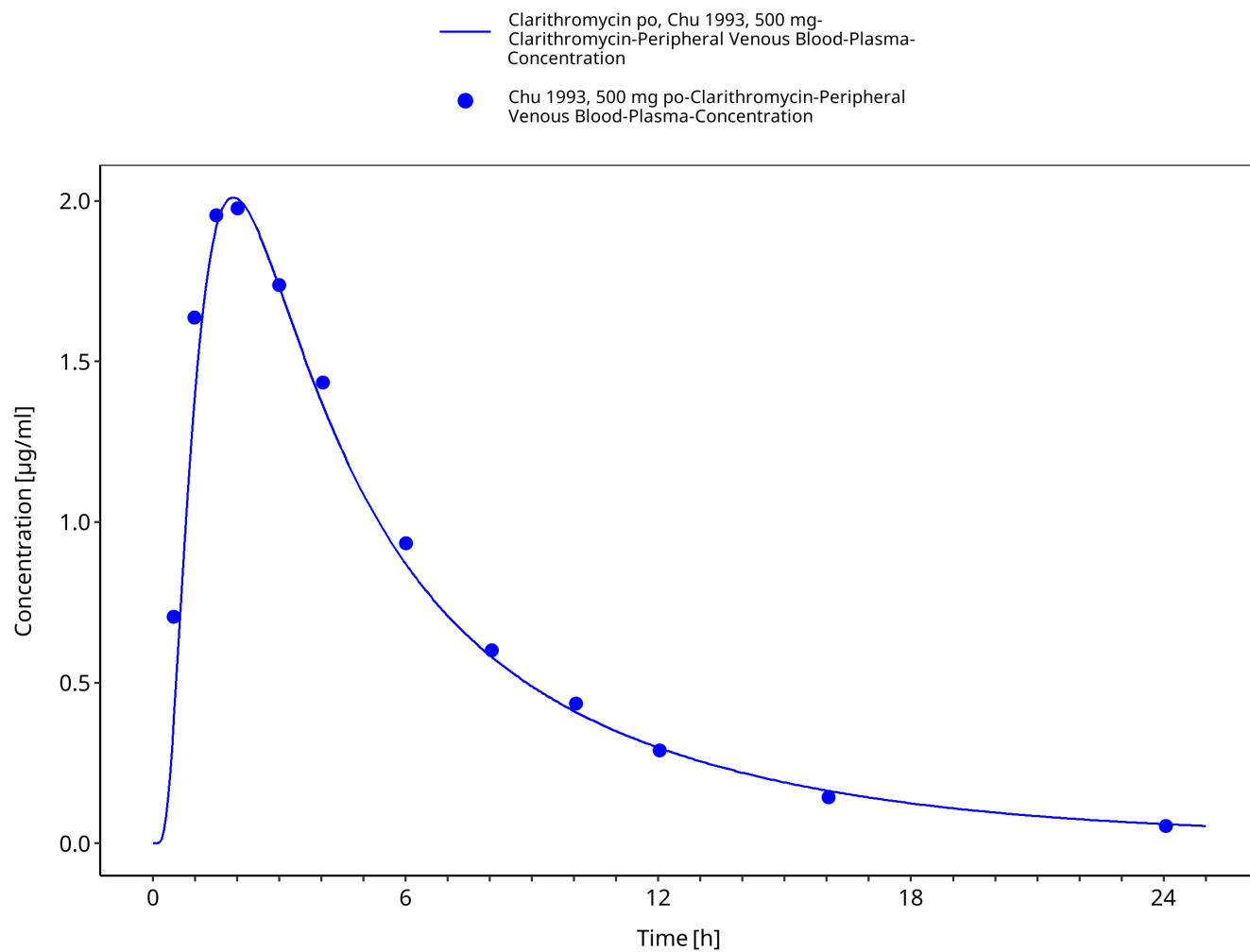


Figure 3-9: Time Profile Analysis

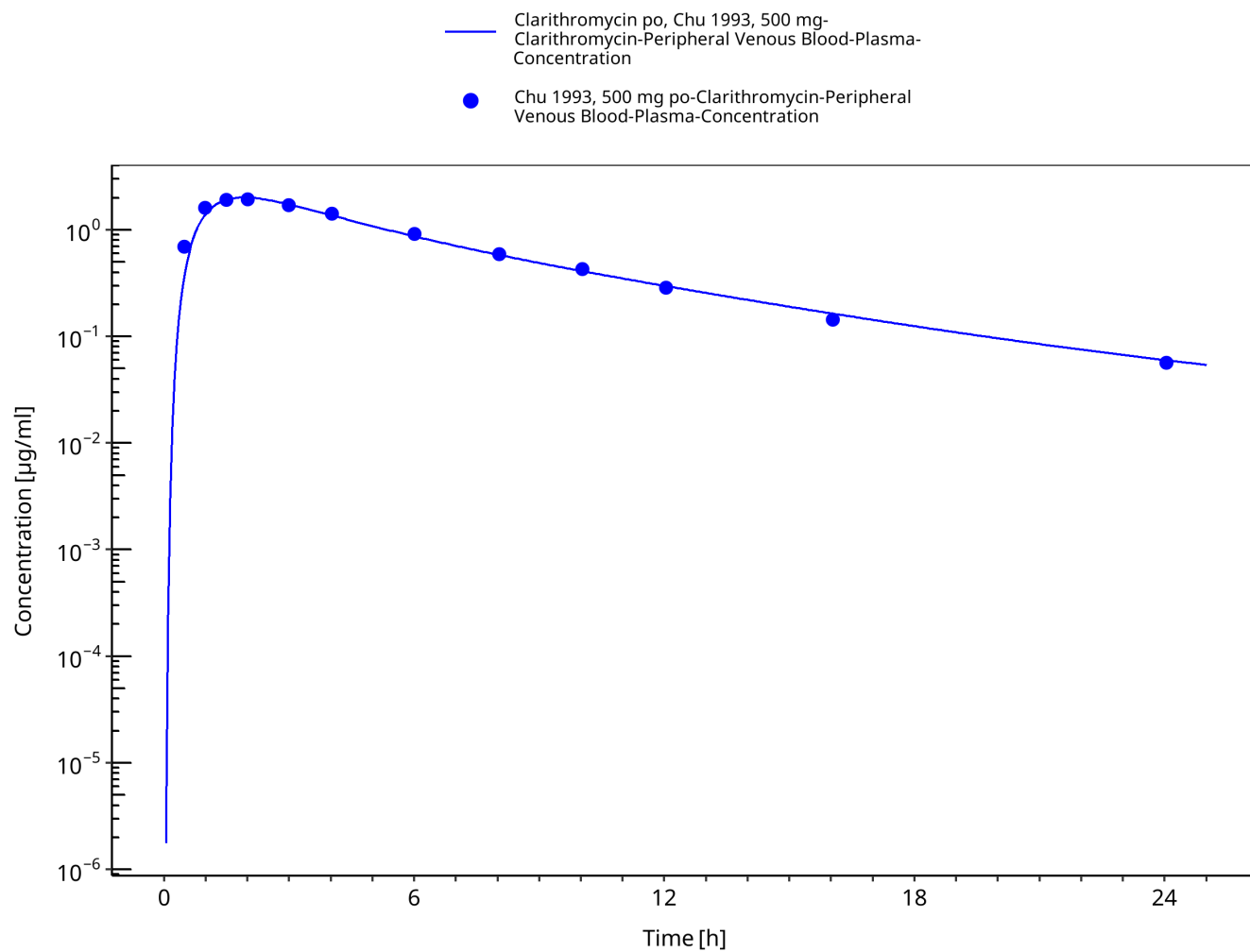


Figure 3-10: Time Profile Analysis 1

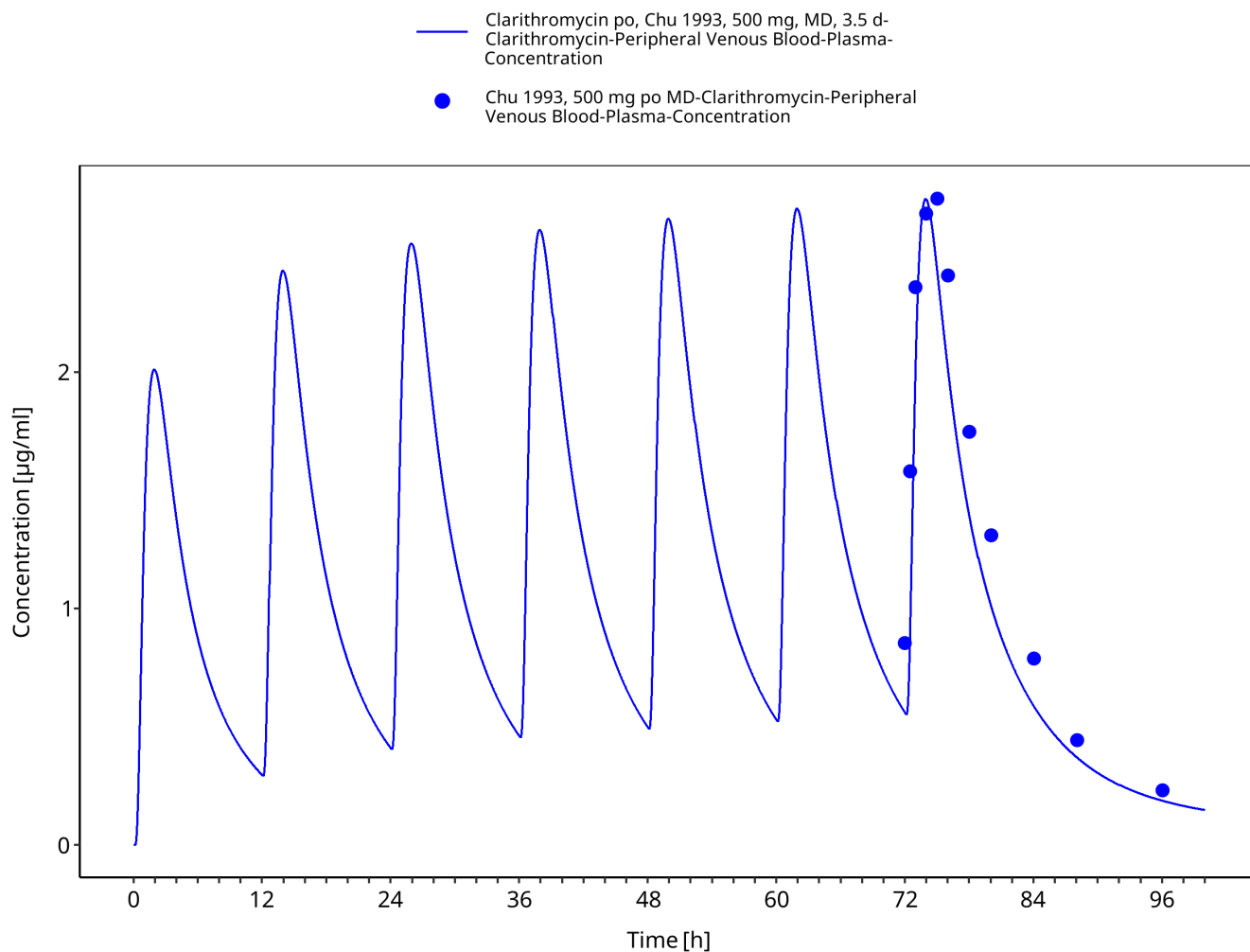


Figure 3-11: Time Profile Analysis

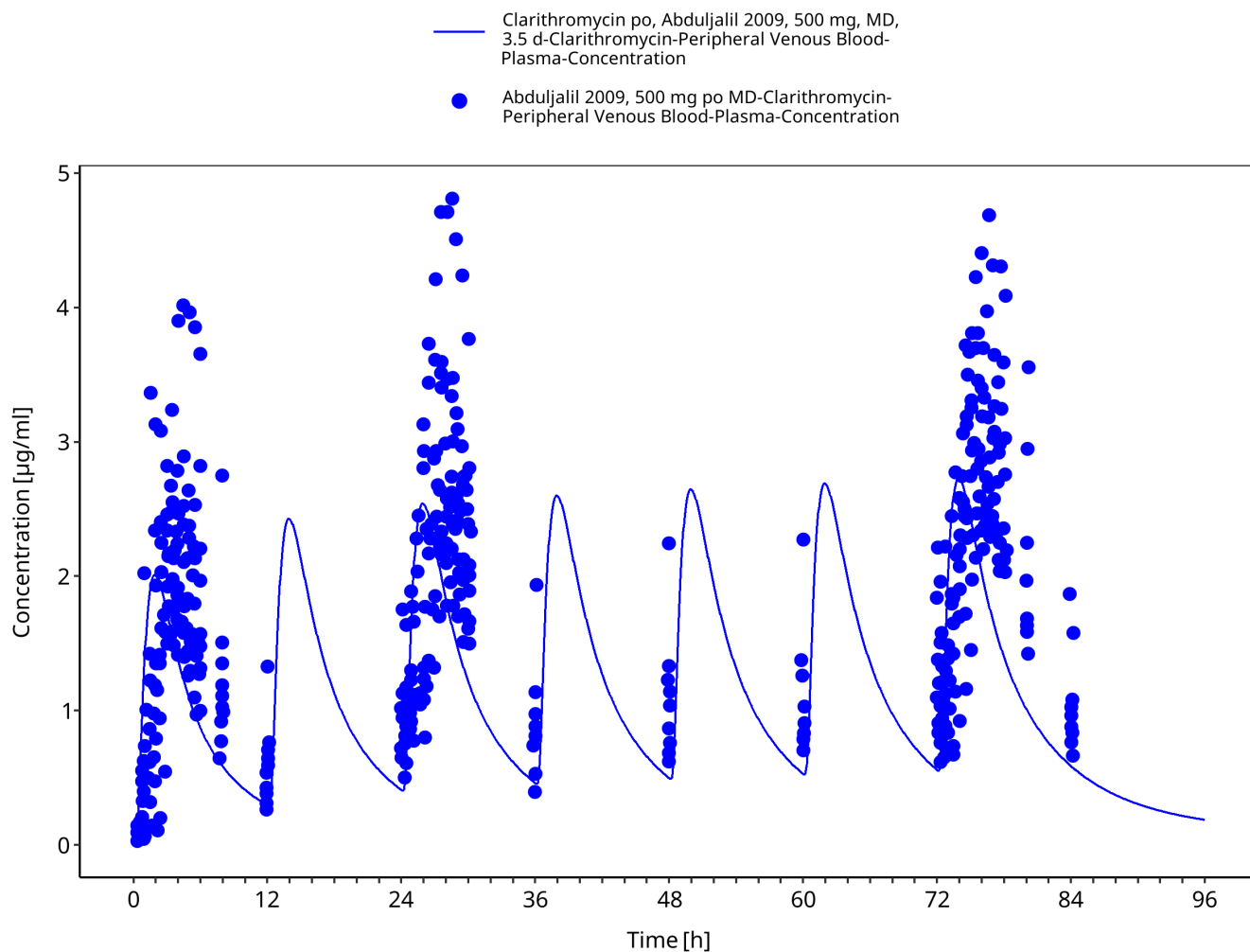


Figure 3-13: Time Profile Analysis

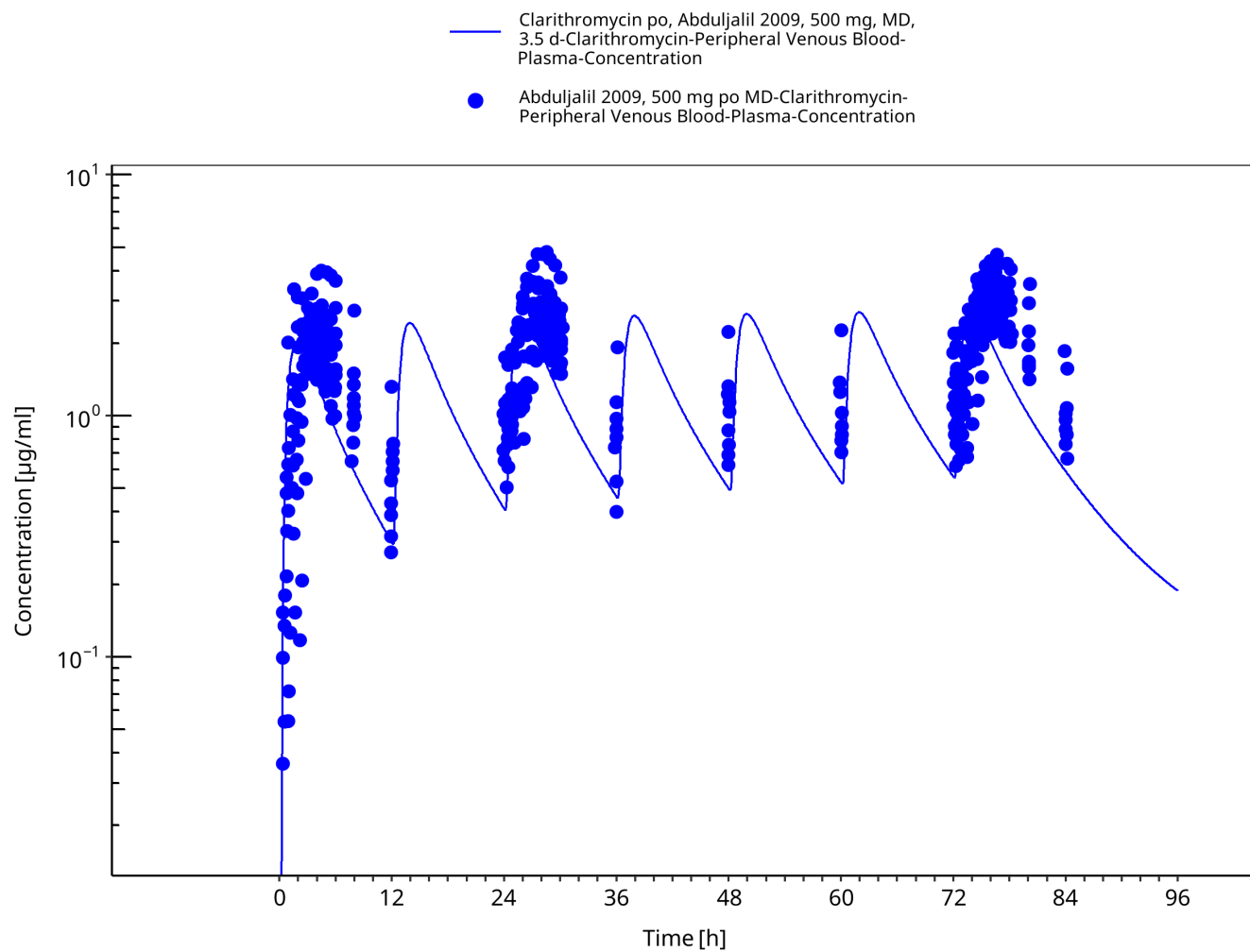


Figure 3-14: Time Profile Analysis 1

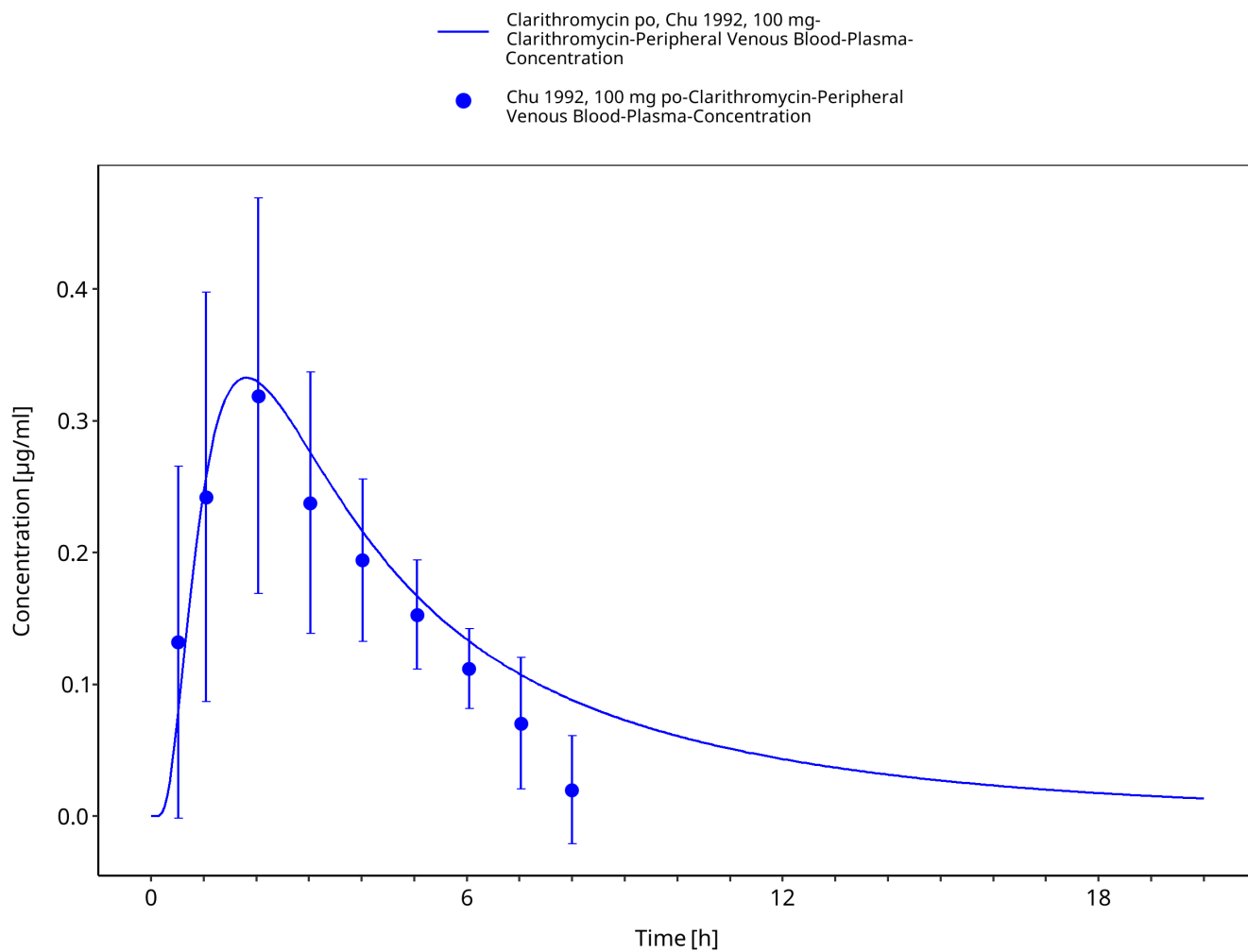


Figure 3-15: Time Profile Analysis

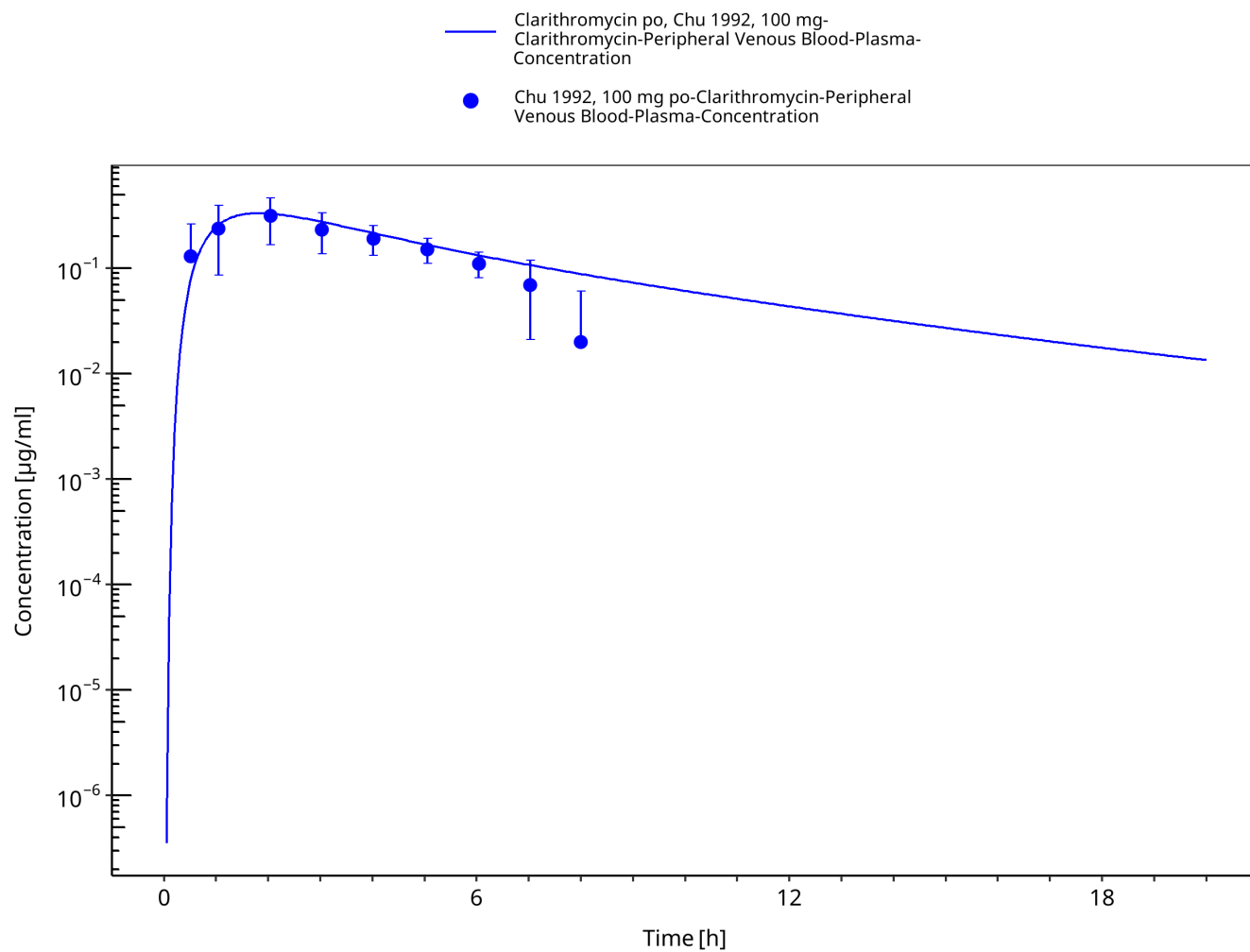


Figure 3-16: Time Profile Analysis 1

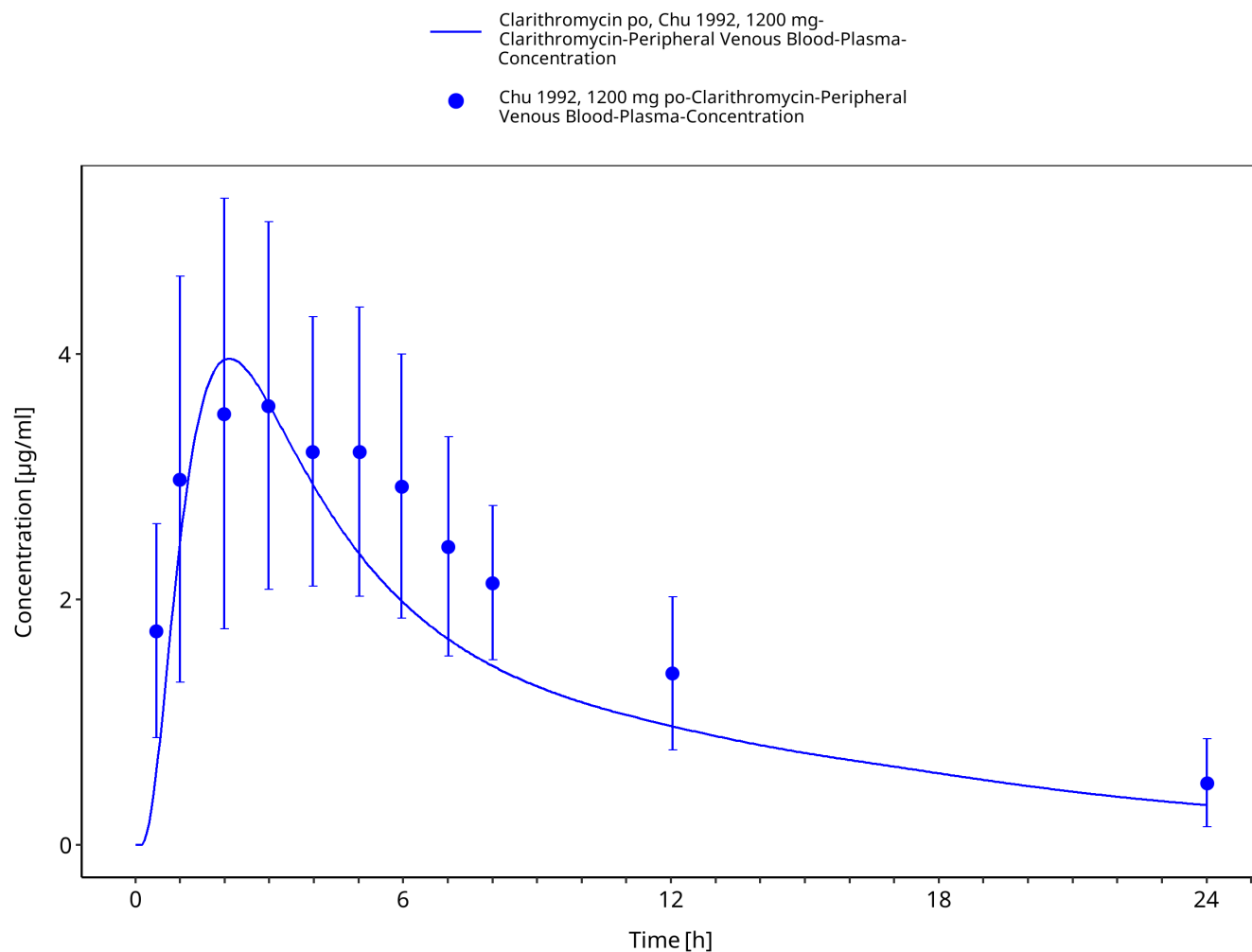


Figure 3-17: Time Profile Analysis

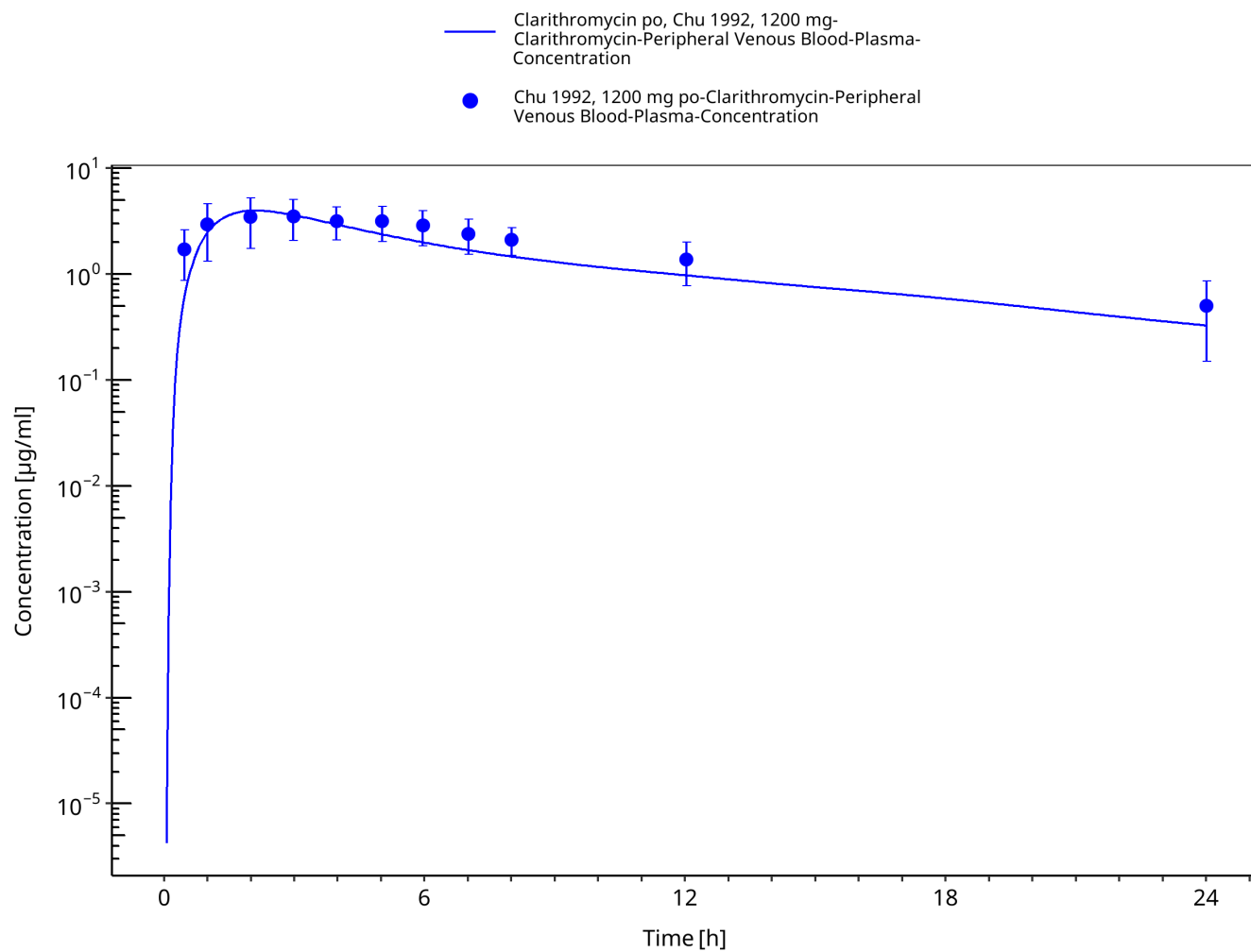


Figure 3-18: Time Profile Analysis 1

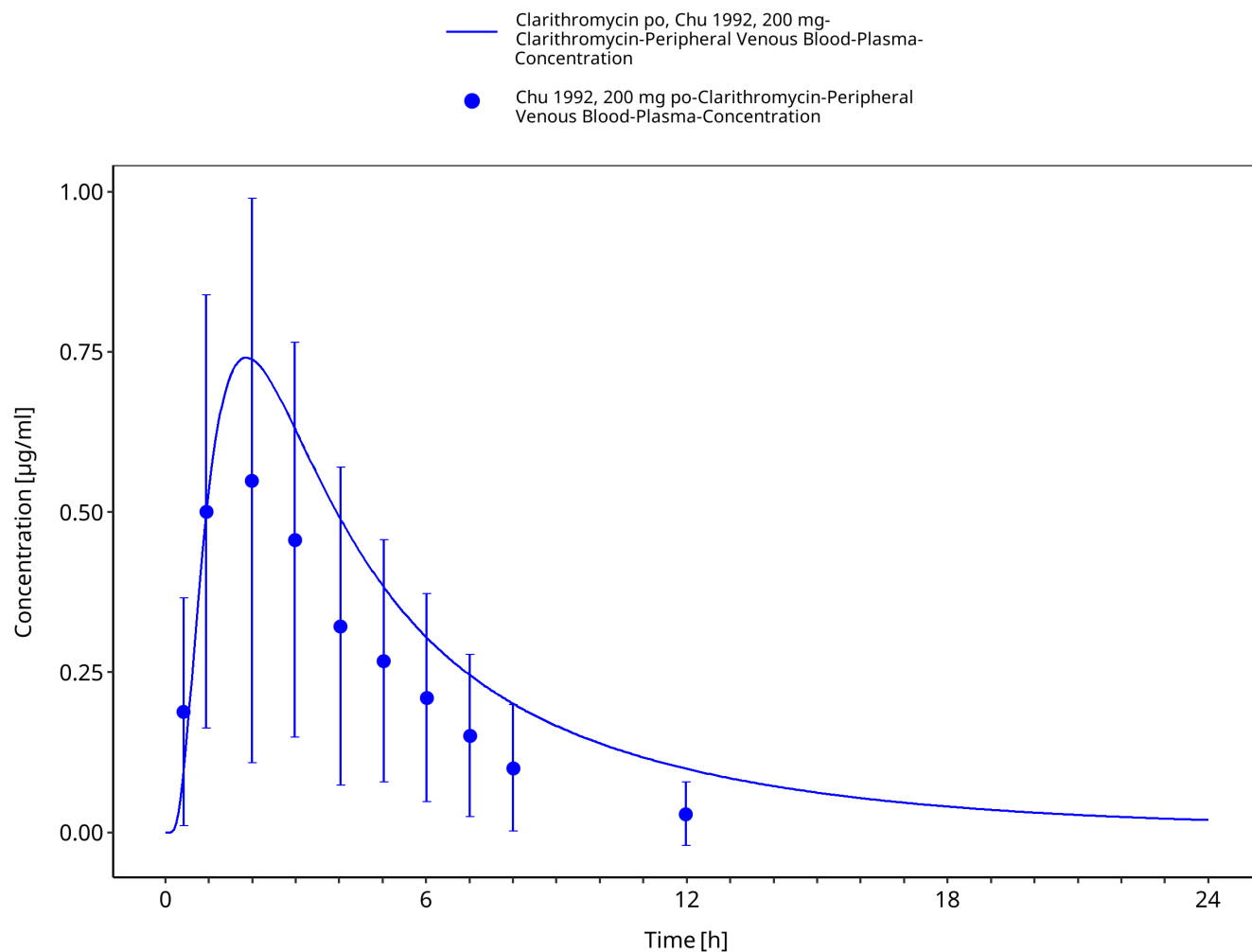


Figure 3-19: Time Profile Analysis

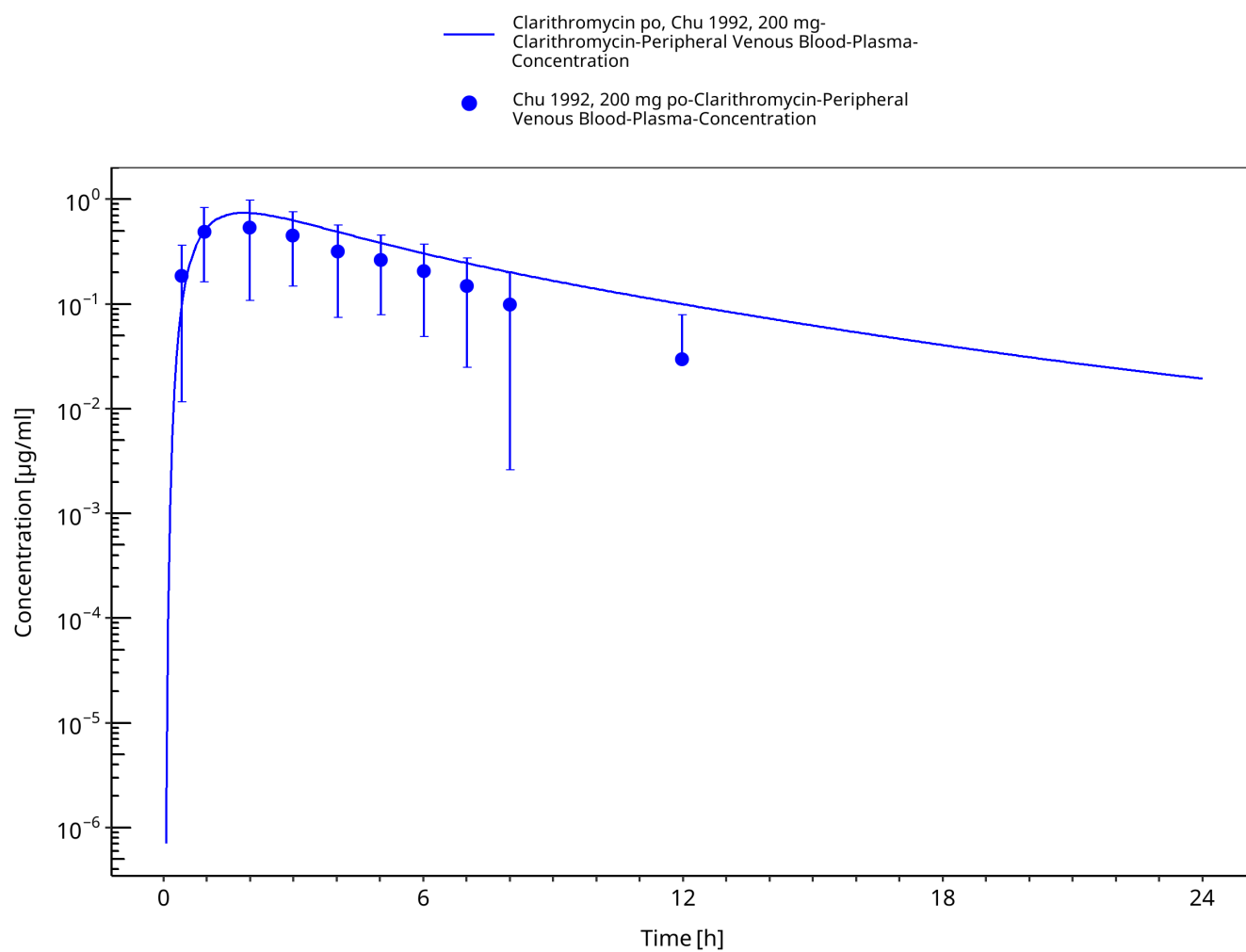


Figure 3-20: Time Profile Analysis 1

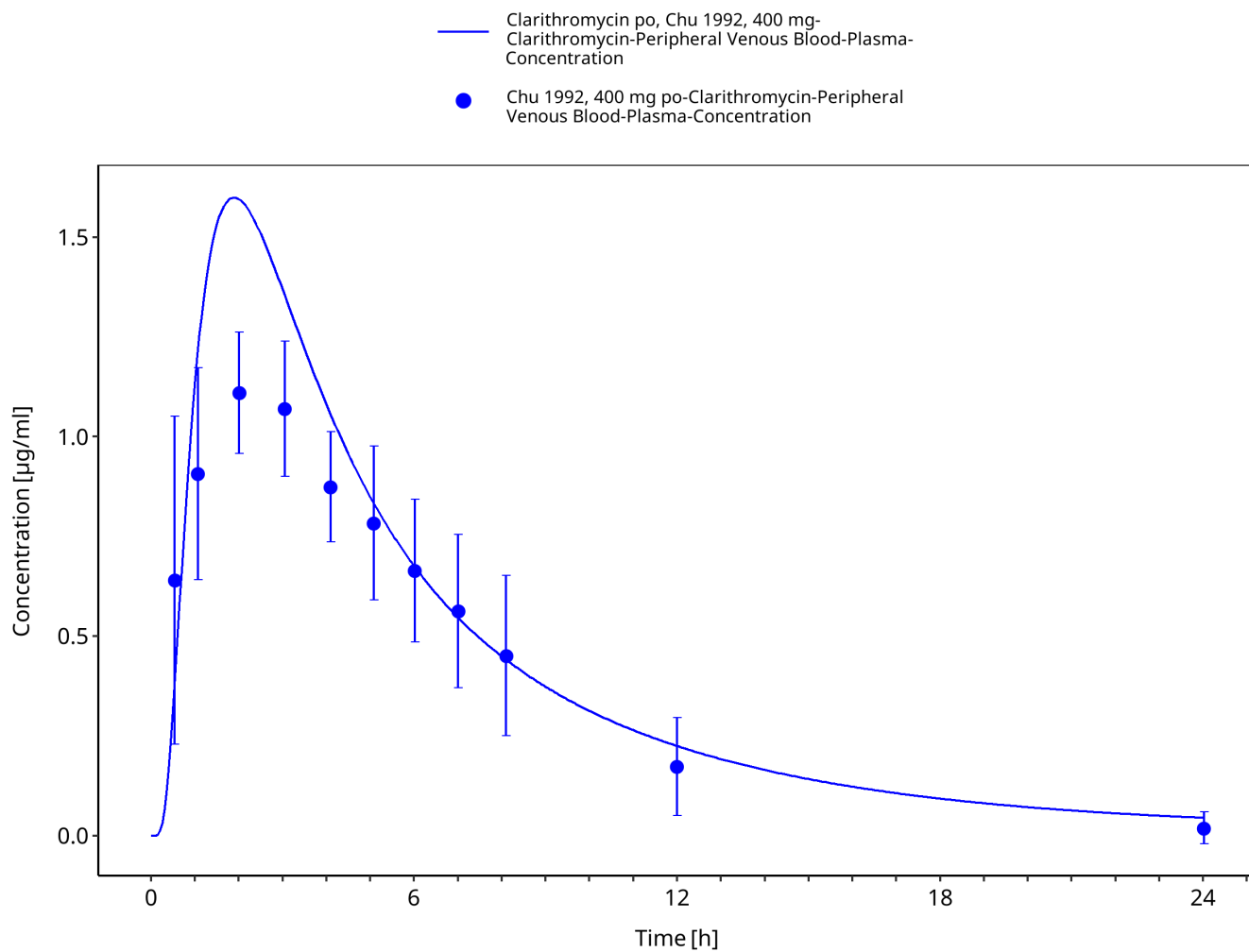


Figure 3-21: Time Profile Analysis

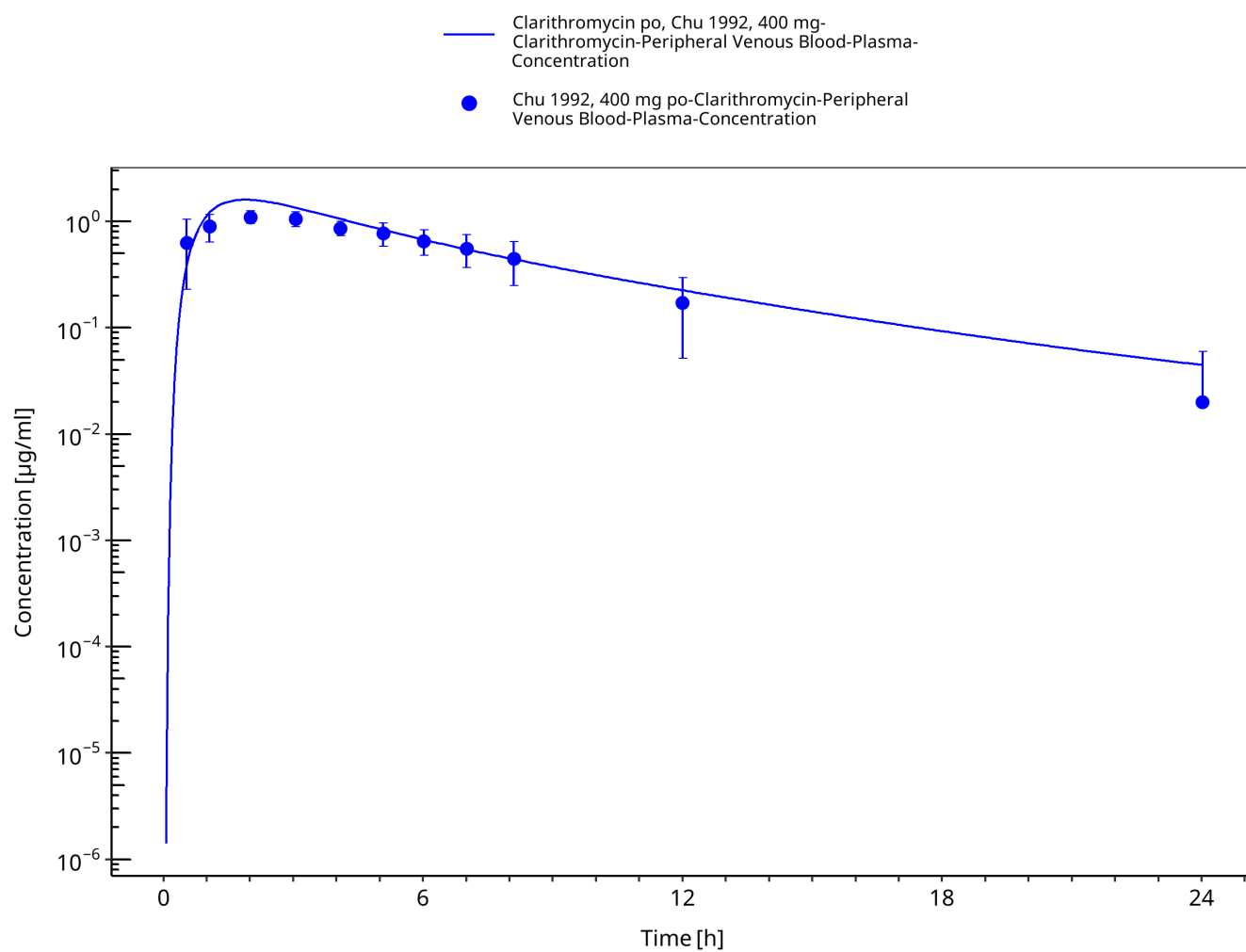


Figure 3-22: Time Profile Analysis 1

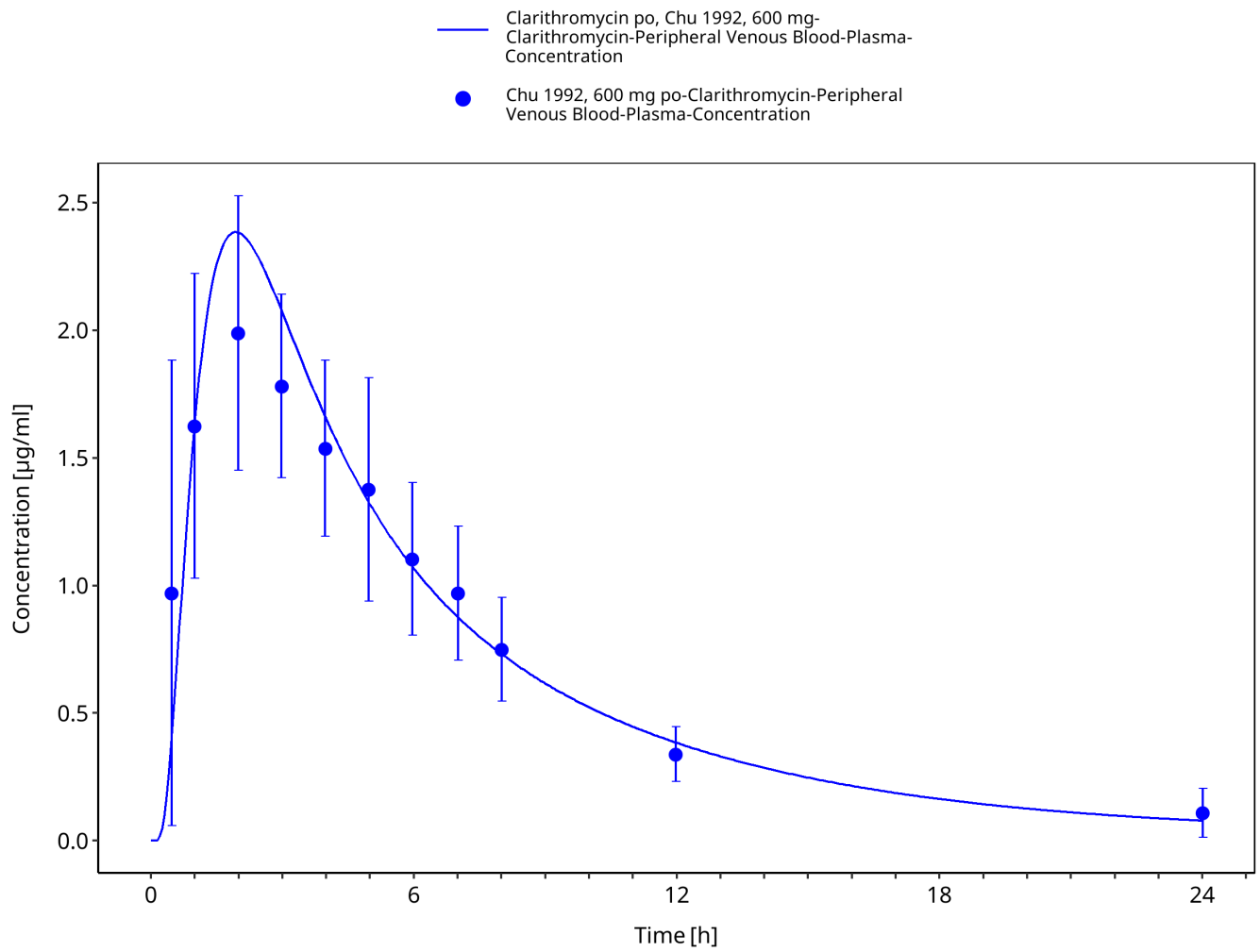


Figure 3-23: Time Profile Analysis

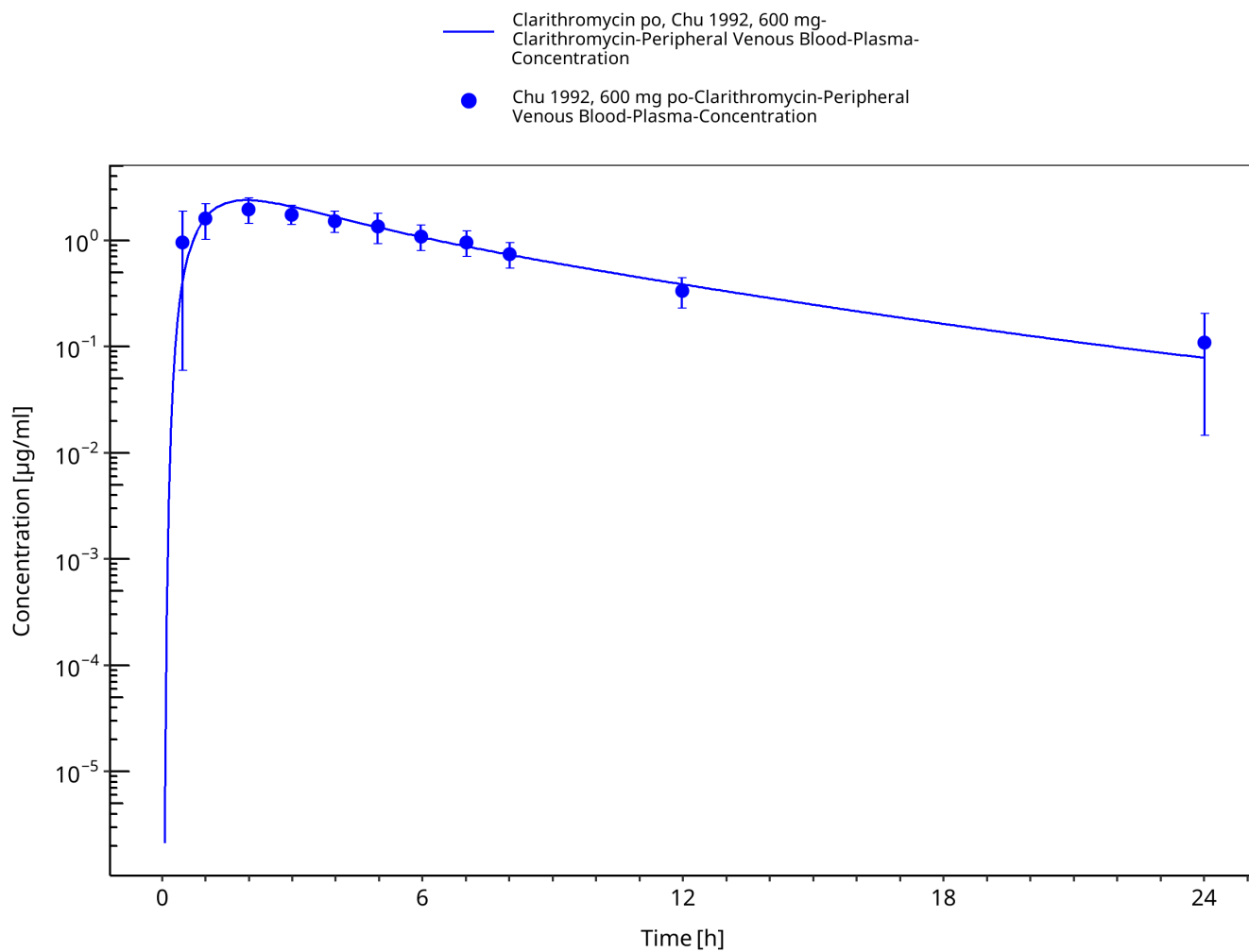


Figure 3-24: Time Profile Analysis 1

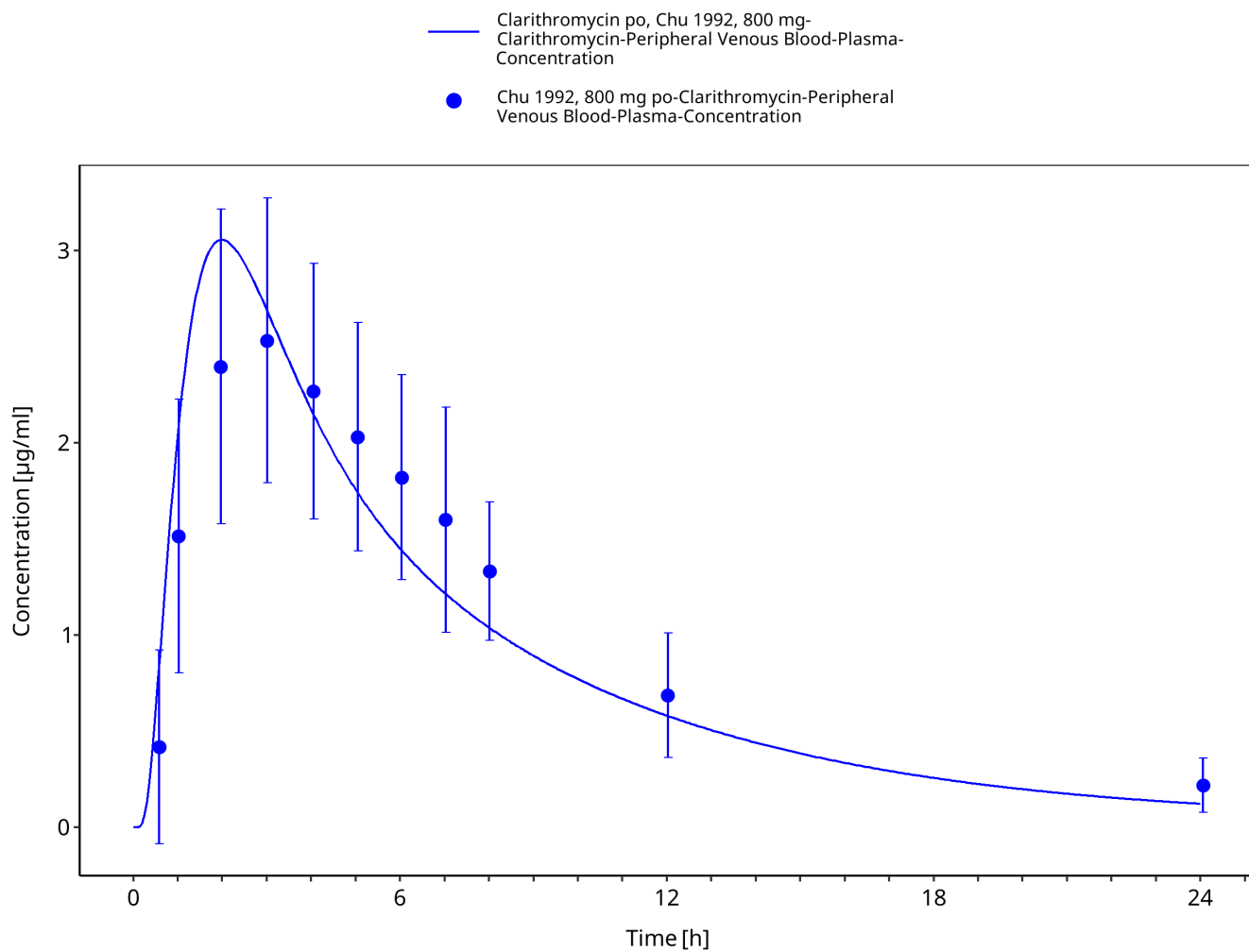


Figure 3-25: Time Profile Analysis

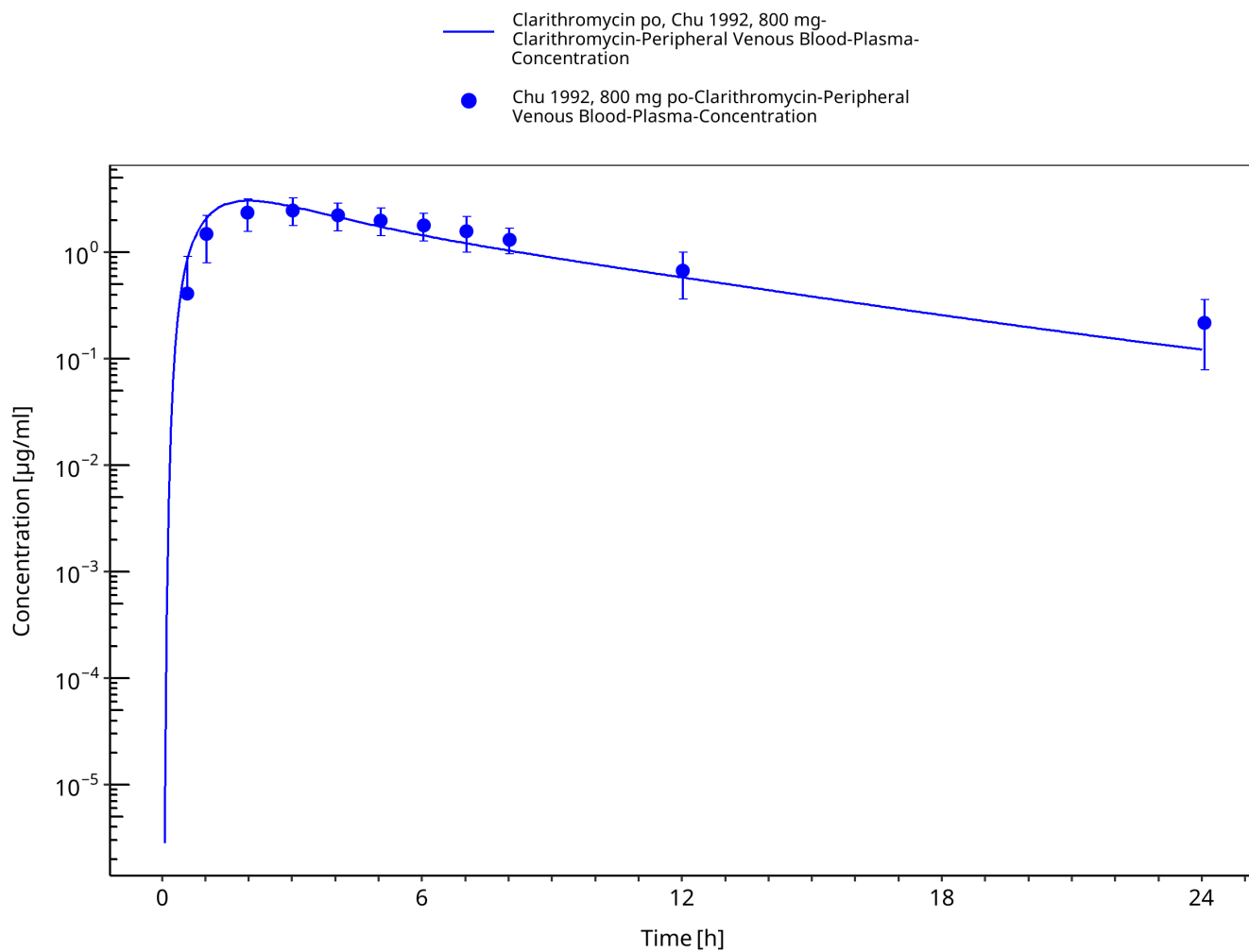


Figure 3-26: Time Profile Analysis 1

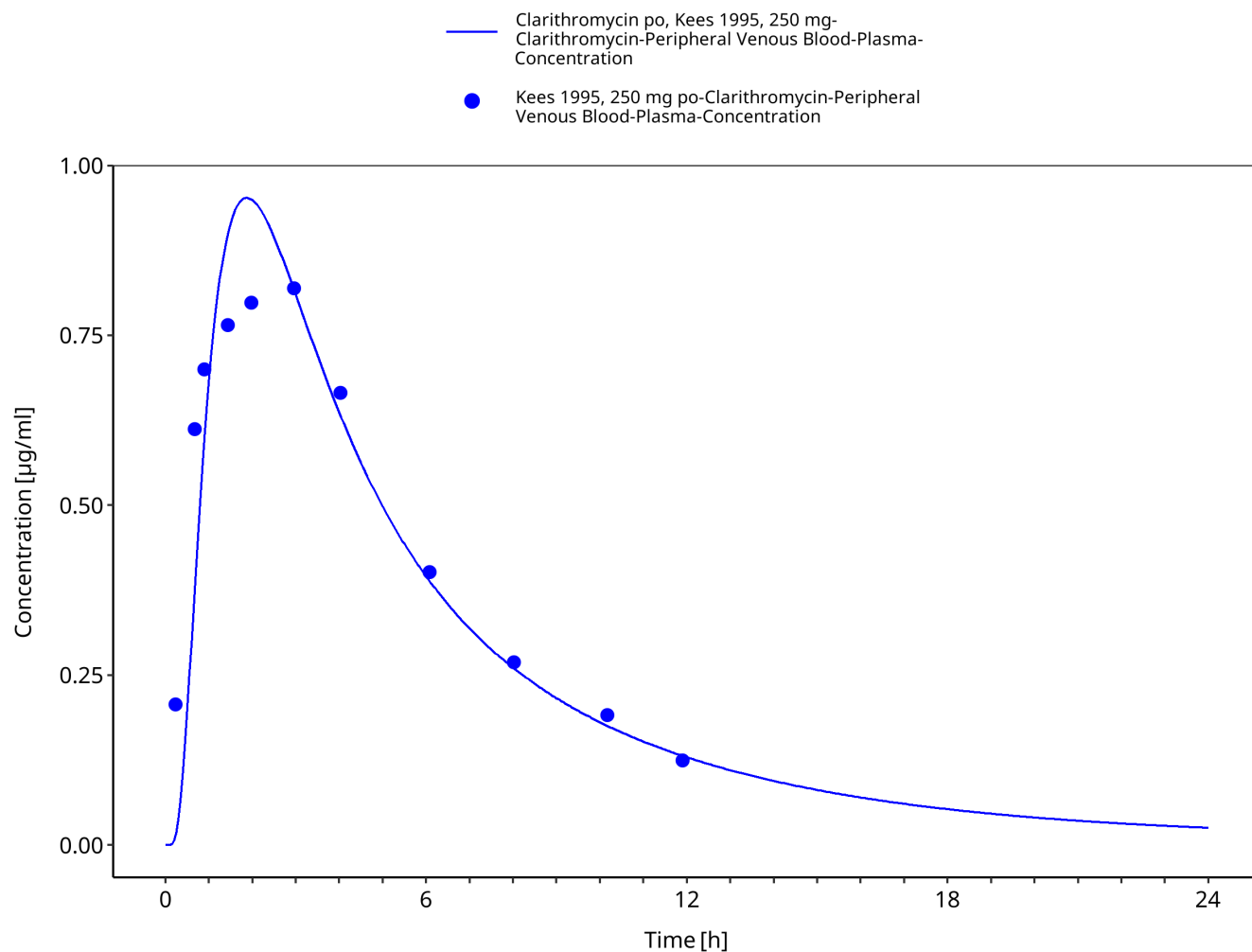


Figure 3-27: Time Profile Analysis

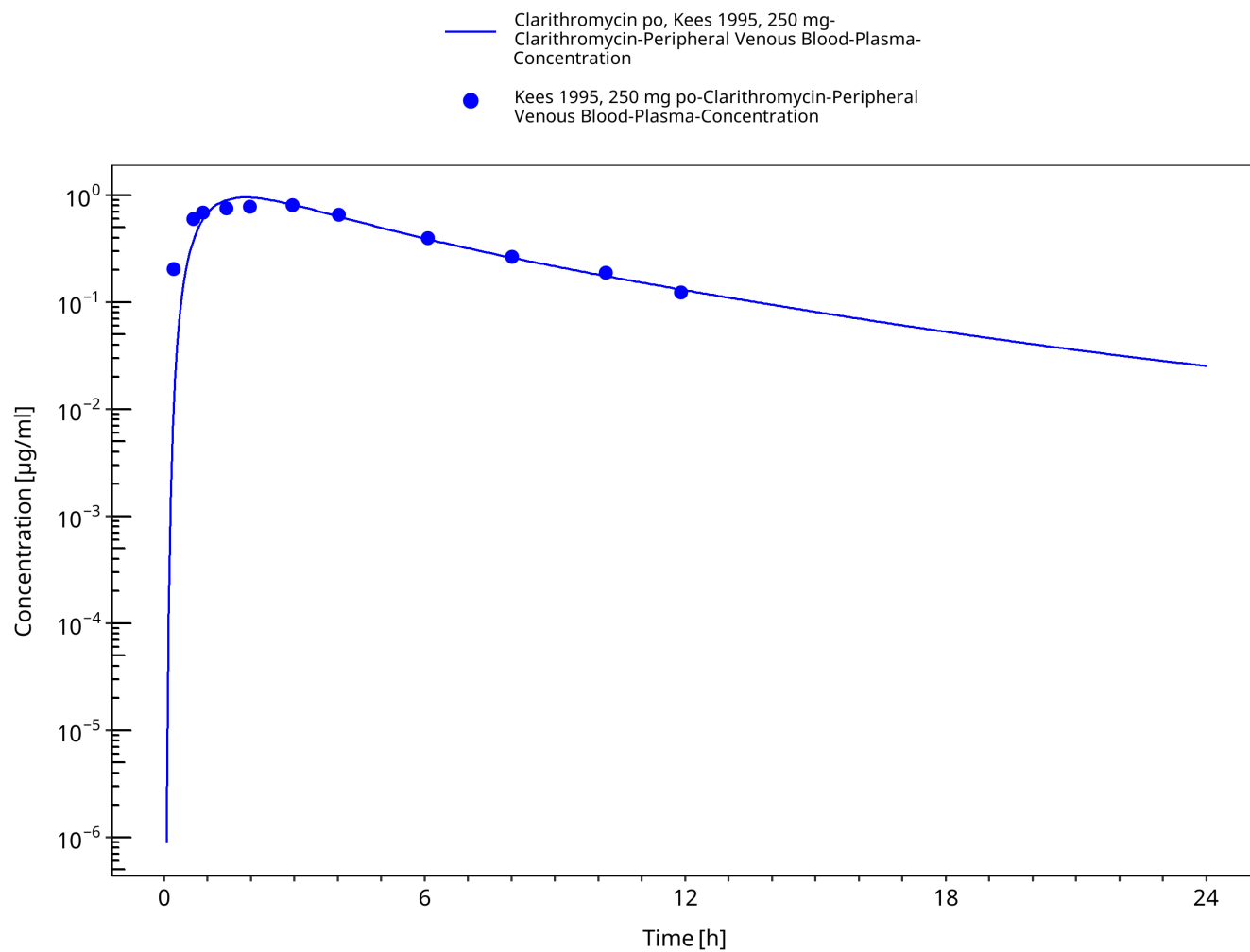


Figure 3-28: Time Profile Analysis 1

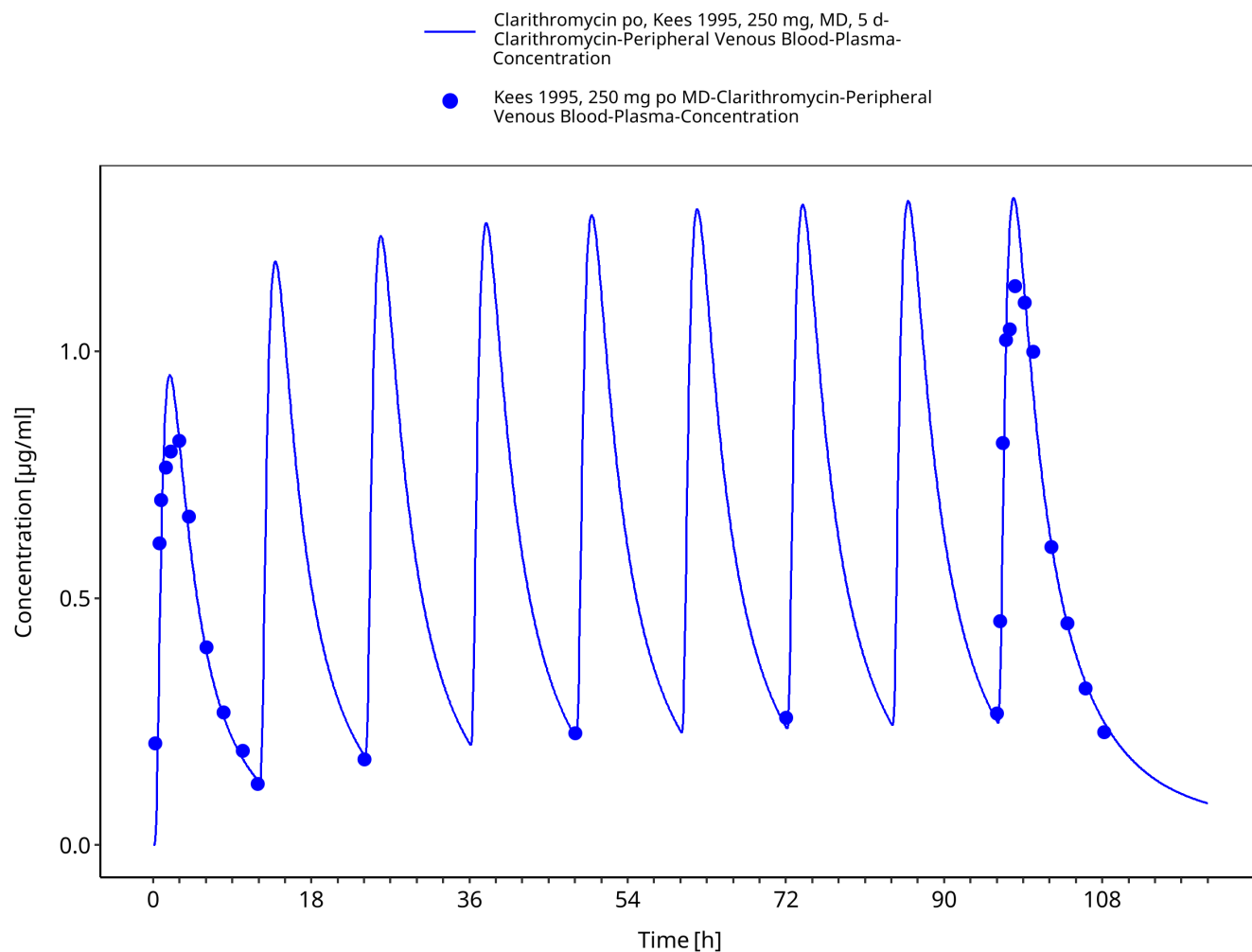


Figure 3-29: Time Profile Analysis

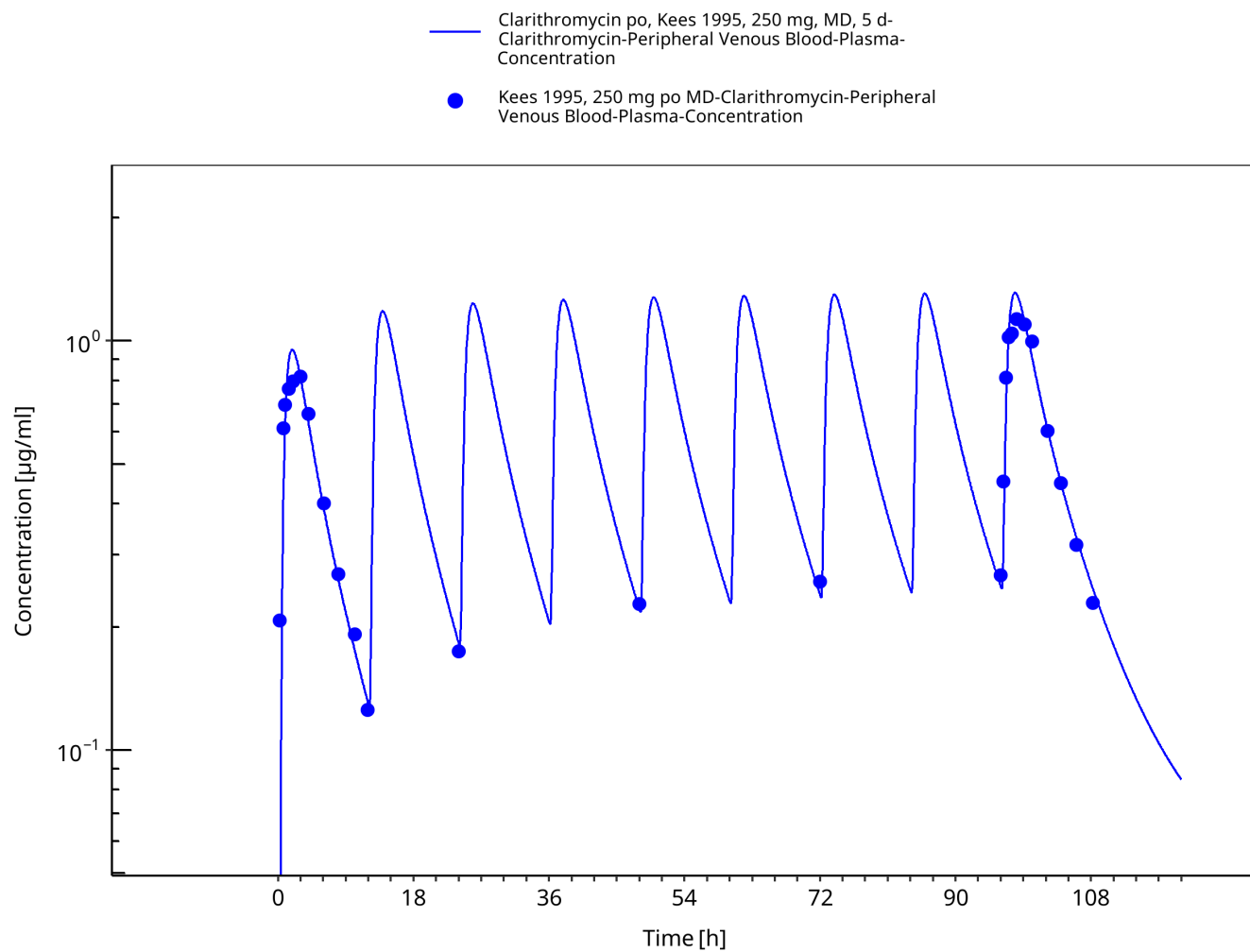


Figure 3-30: Time Profile Analysis 1

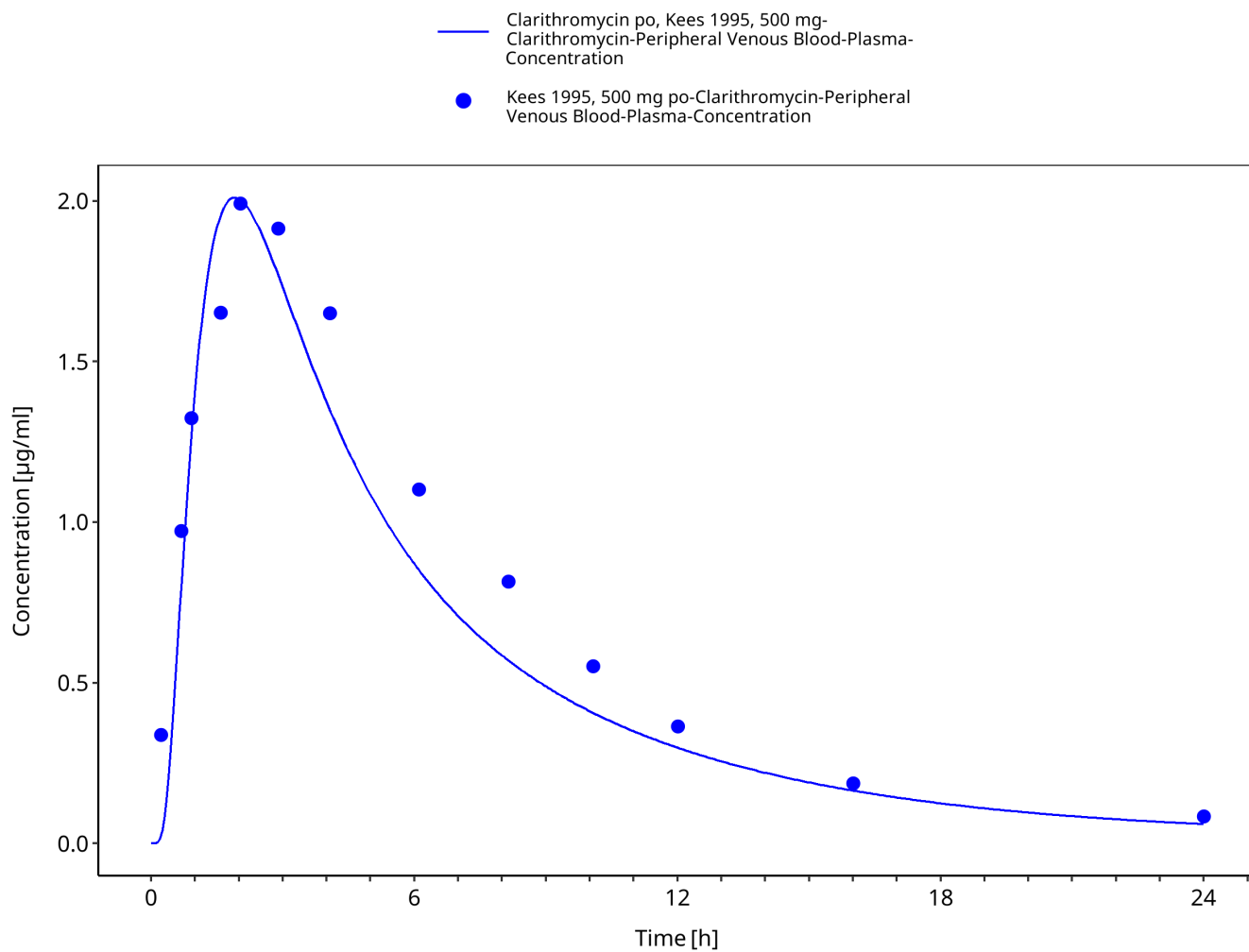


Figure 3-31: Time Profile Analysis

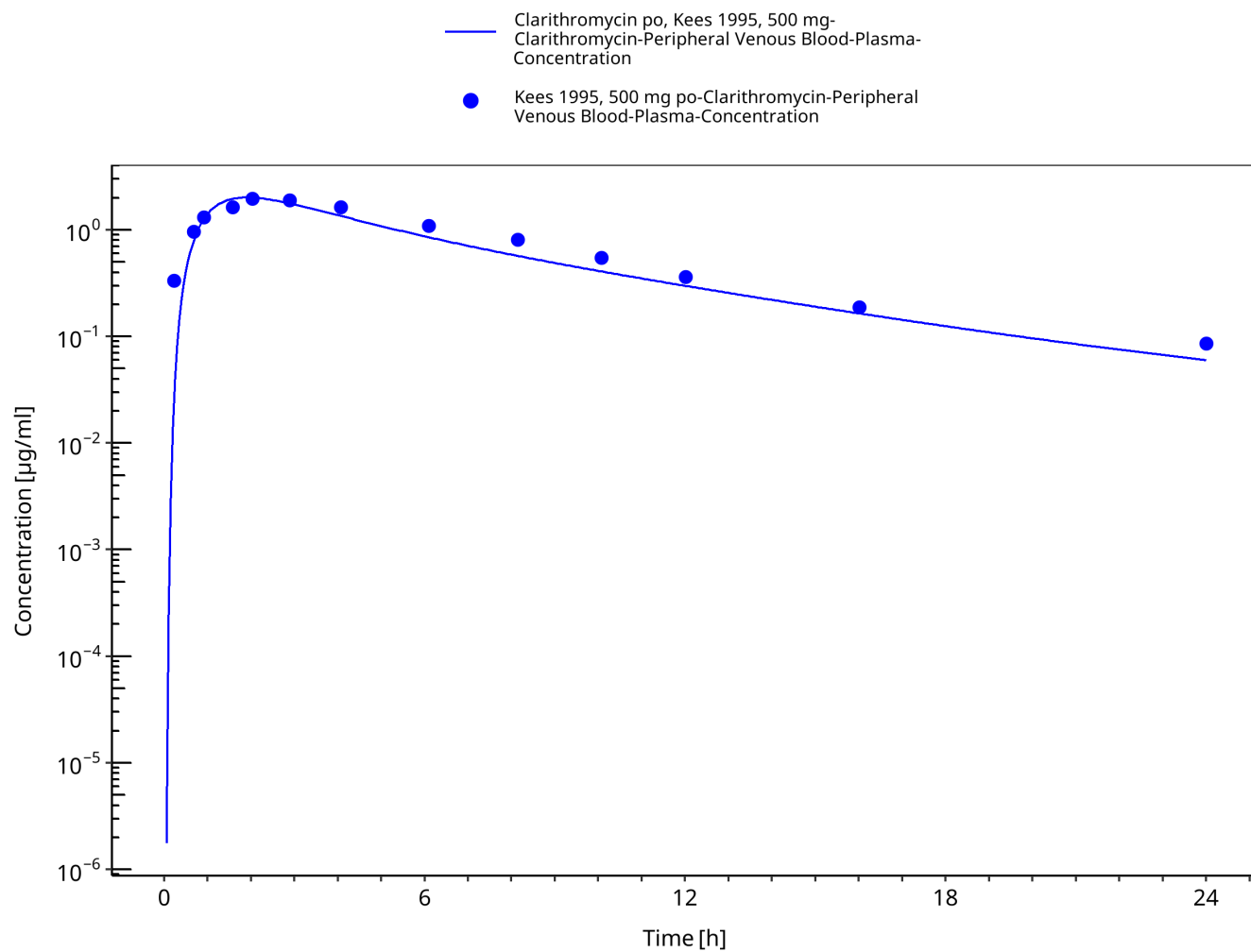


Figure 3-32: Time Profile Analysis 1

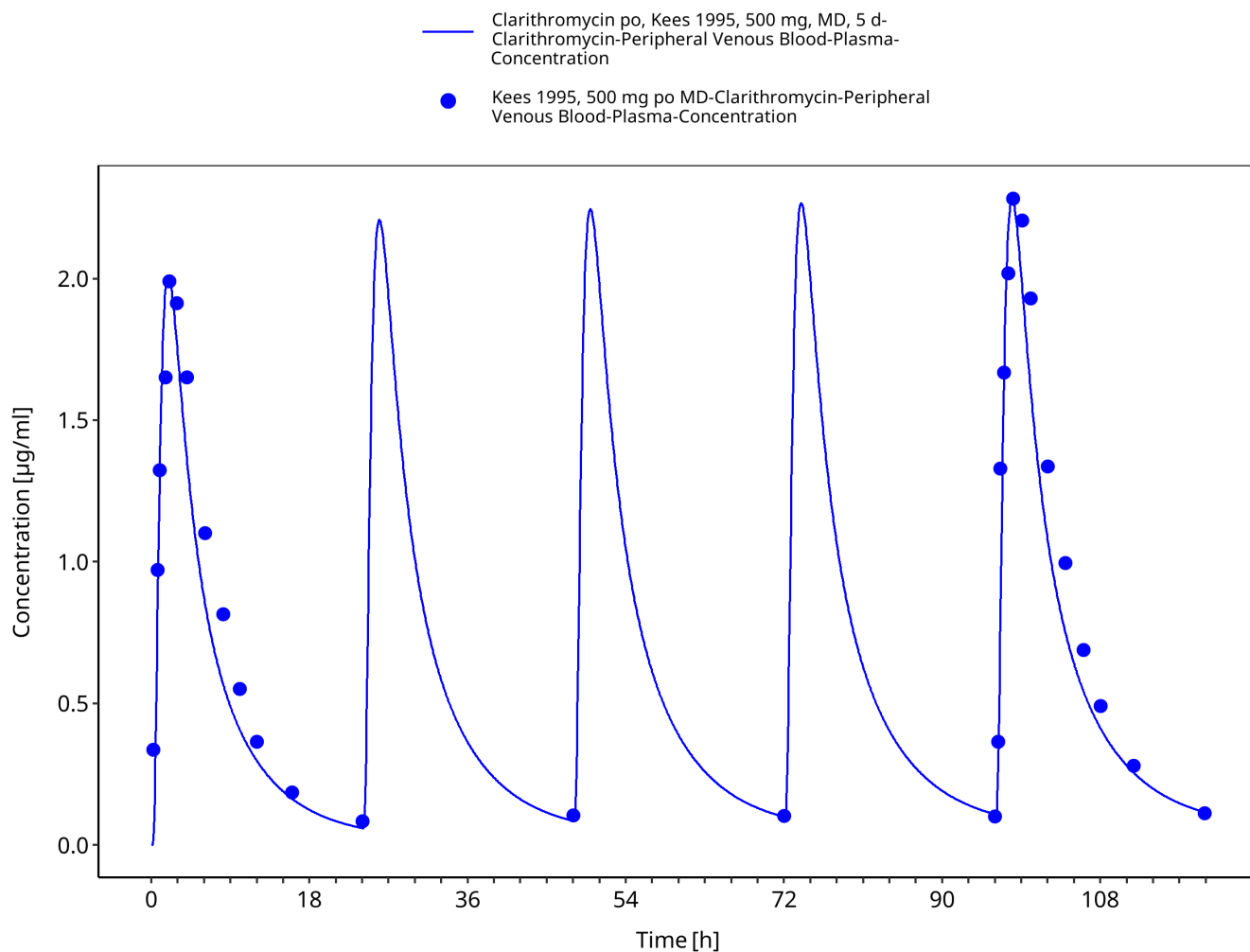


Figure 3-33: Time Profile Analysis

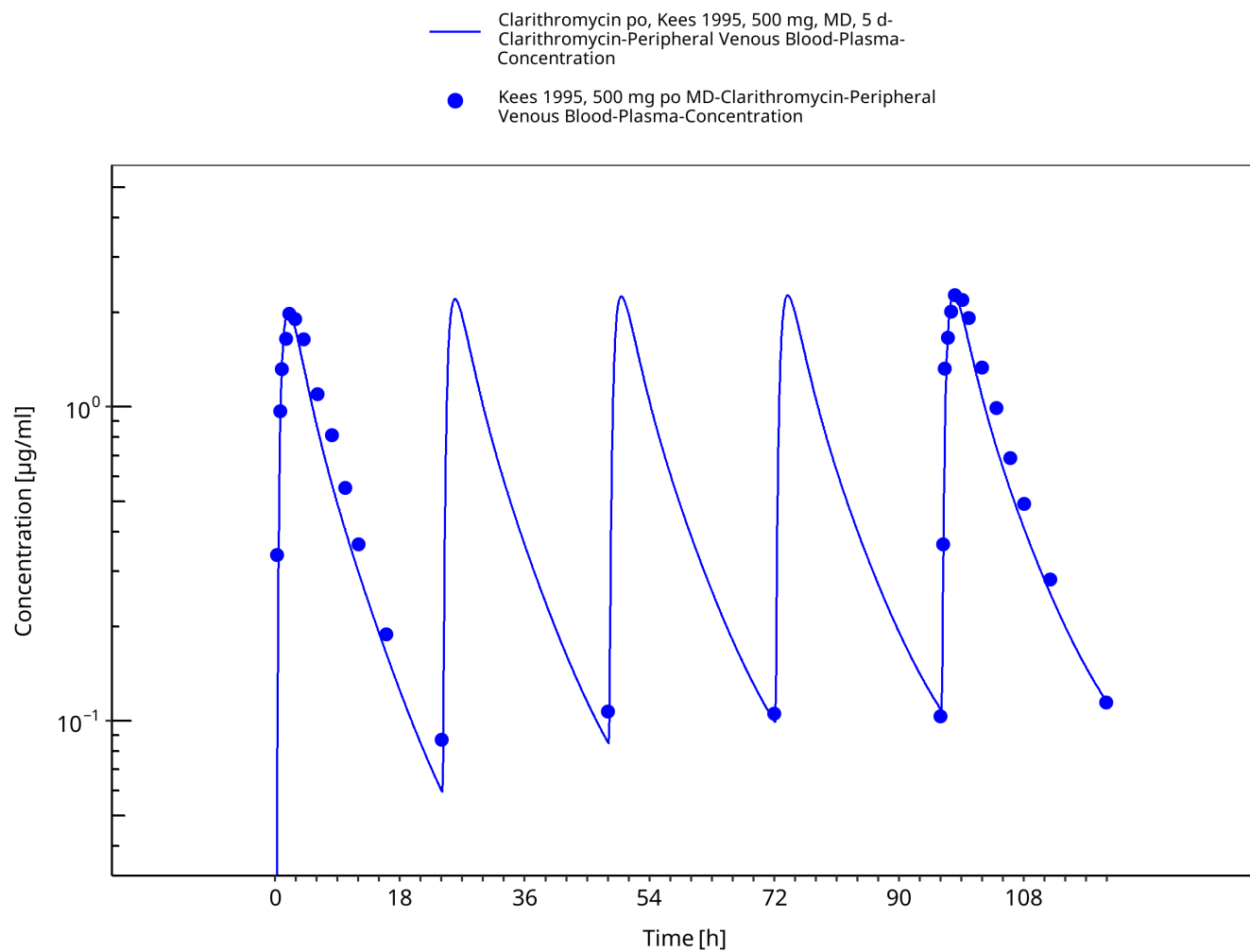


Figure 3-34: Time Profile Analysis 1

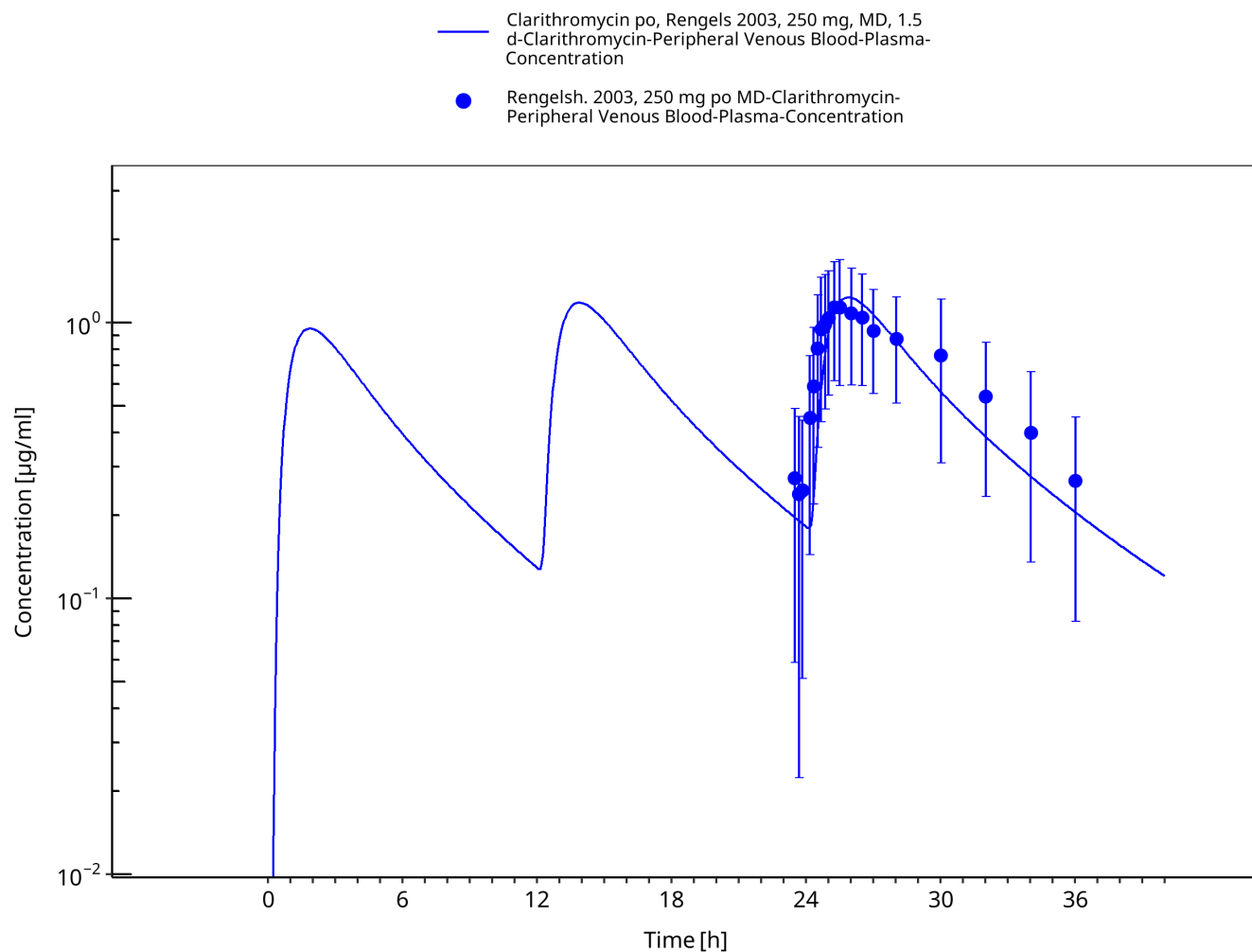


Figure 3-36: Time Profile Analysis 1

4 Conclusion

The herein presented PBPK model adequately describes the pharmacokinetics of clarithromycin in adults. In particular, it applies increased transfer and accumulation in red blood cells, metabolism by CYP3A4, renal clearance as unchanged drug and mechanism-based inactivation of CYP3A4. Thus, the model is fit for purpose to be applied for the investigation of drug-drug interactions with regard to inhibition of CYP3A4 and P-gp.

5 References

- Abduljalil 2009** Abduljalil, K. et al. Modeling the autoinhibition of clarithromycin metabolism during repeated oral administration. *Antimicrob. Agents Chemother.* 53, 2892–901 (2009).
- Chu 1992a** Chu, S.Y. et al. Pharmacokinetics of clarithromycin, a new macrolide, after single ascending oral doses. *Antimicrob. Agents Chemother.* 36, 2447–53 (1992).
- Chu 1992b** Chu, S.Y., Deaton, R. & Cavanaugh, J. Absolute bioavailability of clarithromycin after oral administration in humans. *Antimicrob. Agents Chemother.* 36, 1147–50 (1992).
- Chu 1993a** Chu, S. et al. Single- and multiple-dose pharmacokinetics of clarithromycin, a new macrolide antimicrobial. *J. Clin. Pharmacol.* 33, 719–26 (1993).
- Chu 1993b** Chu, S.Y. et al. Effect of moderate or severe hepatic impairment on clarithromycin pharmacokinetics. *J. Clin. Pharmacol.* 33, 480–5 (1993).
- Davey 1991** Davey, P.G. The pharmacokinetics of clarithromycin and its 14-OH metabolite. *J. Hosp. Infect.* 19 Suppl A, 29–37 (1991).
- drugbank.ca.** (<https://www.drugbank.ca/drugs/DB01211>), accessed on 04-28-2020.
- Eberl 2007** Eberl, S. et al. Role of p-glycoprotein inhibition for drug interactions: evidence from in vitro and pharmacoepidemiological studies. *Clin. Pharmacokinet.* 46, 1039–49 (2007).
- Hanke 2018** Hanke, N. et al. PBPK Models for CYP3A4 and P-gp DDI Prediction: A Modeling Network of Rifampicin, Itraconazole, Clarithromycin, Midazolam, Alfentanil, and Digoxin. *CPT Pharmacometrics Syst. Pharmacol.* 7, 647–659 (2018)
- Ishiguro 1989** Ishiguro M, Koga H, Kohno S, Hayashi T, Yamaguchi K, Hirota M. Penetration of macrolides into human polymorphonuclear leucocytes. *J Antimicrob Chemother.* 24, 719–29 (1989)
- Ito 2003** Ito, K., Ogihara, K., Kanamitsu, S.-I. & Itoh, T. Prediction of the in vivo interaction between midazolam and macrolides based on in vitro studies using human liver microsomes. *Drug Metab. Dispos.* 31, 945–54 (2003).
- Kees 1995** Kees, F., Wellenhofer, M. & Grobecker, H. Serum and cellular pharmacokinetics of clarithromycin 500 mg q.d. and 250 mg b.i.d. in volunteers. *Infection* 23, 168–72 (1995).
- Kuepfer 2016** Kuepfer L, Niederalte C, Wendl T, Schlender JF, Willmann S, Lippert J, Block M, Eissing T, Teutonico D. Applied Concepts in PBPK Modeling: How to Build a PBPK/PD Model. *CPT Pharmacometrics Syst Pharmacol.* 2016 Oct;5(10):516–531. doi: 10.1002/psp4.12134. Epub 2016 Oct 19.
- Lappin 2011** Lappin, G. et al. Comparative pharmacokinetics between a microdose and therapeutic dose for clarithromycin, sumatriptan, propafenone, paracetamol (acetaminophen), and phenobarbital in human volunteers. *Eur. J. Pharm. Sci.* 43, 141–50 (2011).
- Mayhew 2000** Mayhew, B.S., Jones, D.R. & Hall, S.D. An in vitro model for predicting in vivo inhibition of cytochrome P450 3A4 by metabolic intermediate complex formation. *Drug Metab. Dispos.* 28, 1031–7 (2000).
- McFarland 1997** McFarland, J.W. et al. Quantitative structure-activity relationships among macrolide antibacterial agents: in vitro and in vivo potency against *Pasteurella multocida*. *J. Med. Chem.* 40, 1340–6 (1997).
- Moj 2017** Moj, D. et al. Clarithromycin, midazolam, and digoxin: application of PBPK modeling to gain new insights into drug-drug interactions and co-medication regimens. *AAPS J.* 19, 298–312 (2017).
- Noreddin 2002** Noreddin, A.M. et al. Pharmacodynamic modeling of clarithromycin against macrolide-resistant [PCR-positive *mef(A)* or *erm(B)*] *Streptococcus pneumoniae* simulating clinically achievable serum and epithelial lining fluid free-

drug concentrations. *Antimicrob. Agents Chemother.* 46, 4029–34 (2002).

PK-Sim Ontogeny Database Version 7.3 (<https://github.com/Open-Systems-Pharmacology/OSPSuite.Documentation/blob/38cf71b384cfc25cfa0ce4d2f3addfd32757e13b/PK-Sim%20Ontogeny%20Database%20Version%207.3.pdf>)

Polasek 2006 Polasek, T.M. & Miners, J.O. Quantitative prediction of macrolide drug-drug interaction potential from in vitro studies using testosterone as the human cytochrome P4503A substrate. *Eur. J. Clin. Pharmacol.* 62, 203–8 (2006).

Rengelshausen 2003 Rengelshausen, J. et al. Contribution of increased oral bioavailability and reduced nonglomerular renal clearance of digoxin to the digoxin-clarithromycin interaction. *Br. J. Clin. Pharmacol.* 56, 32–8 (2003).

Rodrigues 1997 Rodrigues, A.D., Roberts, E.M., Mulford, D.J., Yao, Y. & Ouellet, D. Oxidative metabolism of clarithromycin in the presence of human liver microsomes. Major role for the cytochrome P4503A (CYP3A) subfamily. *Drug Metab. Dispos.* 25, 623–30 (1997).

Rodvold 1999 Rodvold, K.A. Clinical pharmacokinetics of clarithromycin. *Clin. Pharmacokinet.* 37, 385–98 (1999).

Salem 2003 Salem, I.I. & Düzgünes, N. Efficacies of cyclodextrin-complexed and liposome-encapsulated clarithromycin against *Mycobacterium avium* complex infection in human macrophages. *Int. J. Pharm.* 250, 403–14 (2003).

Schlender 2016 Schlender JF, Meyer M, Thelen K, Krauss M, Willmann S, Eissing T, Jaehde U. Development of a Whole-Body Physiologically Based Pharmacokinetic Approach to Assess the Pharmacokinetics of Drugs in Elderly Individuals. *Clin Pharmacokinet.* 2016 Dec;55(12):1573-1589.

Seithel 2007 Seithel, A. et al. The influence of macrolide antibiotics on the uptake of organic anions and drugs mediated by OATP1B1 and OATP1B3. *Drug Metab. Dispos.* 35, 779–86 (2007).

Vermeer 2016 Vermeer, L. M., Isringhausen, C. D., Ogilvie, B. W., & Buckley, D. B. Evaluation of ketoconazole and its alternative clinical CYP3A4/5 inhibitors as inhibitors of drug transporters: the in vitro effects of ketoconazole, ritonavir, clarithromycin, and itraconazole on 13 clinically-relevant drug transporters. *Drug Metab. Dispos.* 44, 453–459 (2016).